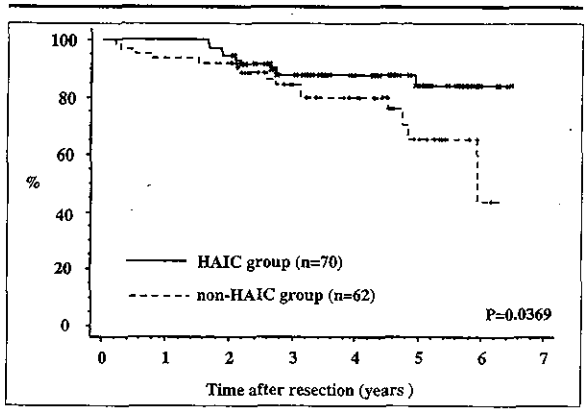

FIGURE 1 Survival curves after curative resection of Dukes C colorectal cancer.

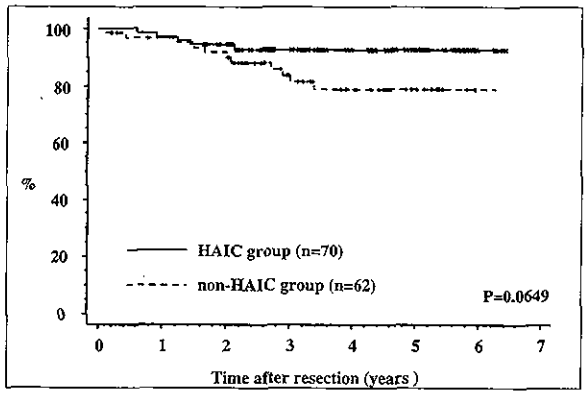

FIGURE 2 Liver metastasis-free curves after curative resection of Dukes C colorectal cancer.

TABLE 3 Location of First Recurrence and Treatment in the Two Groups

		HAIC group (n=70)	Non-HAIC group (n=62)
Location	Liver	5	11
	Lung	7	3
	Brain	1	0
	Local	4	3
	Bone	0	1
	Dissemination	1	1
	Total	18 (25.7%)	19 (30.6%)
Treatment	Surgery	10	9
	Radiation	5	6
	Chemotherapy	0	1
	No treatment	2	2

HAIC group (78.6%) (**Figure 2**). On the other hand, in the cases positive for distant lymph node metastasis, one of the risk factors of liver metastasis of colorectal carcinoma, the cumulative 5-year liver metastasis-free ratio of the HAIC group (91.7%) was significantly higher than that of the non-HAIC group (58.6%, p=0.0268) (**Figure 3**).

DISCUSSION

Approximately 50% of the patients who underwent curative resection for primary colorectal cancer died of metachronous liver metastasis. Reducing the number of such metastases would result in improved survival (11). Most of the many attempts made to do so in previous prospective, randomized trials of adjuvant systemic chemotherapy (6-8) have failed to reduce the development of liver metastasis. It has been suggested that one reason for the lack of success of adjuvant systemic chemotherapy was that sufficiently high doses of drug could not be given because of systemic side effects. Previous researchers have described portal vein infusion of cytotoxic agents at the time of surgery and during the postoperative period as an effective method of preventing metachronous liver metastasis (3,4). However, a large randomized trial of portal vein infusion of fluorouracil and heparin revealed that it had no significant impact on survival (5). Even metastases too small for detection by the naked eye receive a blood supply from newly developed arterioles (12). Ridge *et al.* (13) demonstrated that portal infusion chemotherapy could not maximize drug delivery to hepatic metastases. Daly *et al.* (14) reported significant improvement of tumor response after hepatic artery infusion compared with portal vein infusion. These findings suggest that adjuvant chemotherapy via the hepatic artery is more effective. At the time of initial surgery, micrometastases may already exist in the liver, and if a circulating tumor embolus has caused micrometastasis, portal infusion adjuvant chemotherapy is probably not very effective. Hepatic regional infusion of anticancer drugs achieves high local and low systemic drug concentrations, with the potential for an increased local response rate and decreased systemic toxicity, because the administration of drugs into the hepatic artery may maximize the concentration of the drug in the liver, at least during the first pass through this organ (9,10) and because hepatic extraction and metabolism of the drug will in turn decrease systemic exposure (11).

In this study, the initial regimen was to infuse 5-FU over a five-day period. Because this protocol resulted in many cases of catheter occlusion and the regimen completion rate was only 71.4%, we were obliged to change the protocol to a 24-hour infusion method in 1996. The widely accepted method for effective HAIC administration of 5-FU has been the 5 or 7-day continuous infusion method. However, in 1996, Arai *et al.*

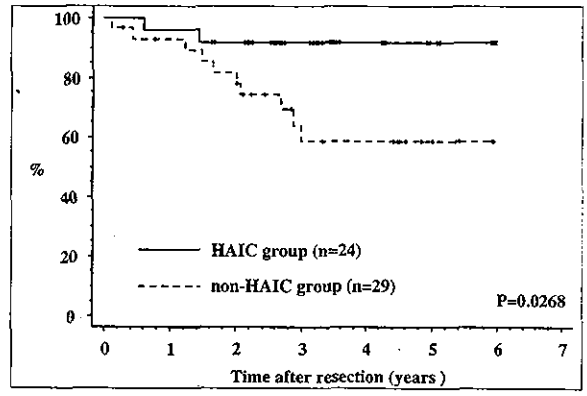

FIGURE 3 Liver metastasis-free curves in distal lymph node positive cases.

(15) reported that a weekly high-dose 5-FU infusion was effective for treating unresectable liver metastases. To treat ambulatory patients safely and to avoid catheter complications at the same time, we decided to alter the drug delivery protocol to the 24-hour infusion method.

In both protocols of this study, systemic toxicity was relatively mild and no patients developed chemical hepatitis or biliary sclerosis. The mean total dose of 5-FU administrated in this course of HAIC was 11.2g and not more than 15g. We assessed the effects of HAIC against patients to whom 7g or more of 5-FU was given, and concluded that 12g of 5-FU could be given without presenting toxicity.

In this study, we found there was an impact on survival after HAIC as a result of decreased liver metastases, especially in the cases positive for distant lymph node metastases. This is a significant finding, because these cases had high potential of developing recurrent tumors in the liver, ultimately leading to death, whereas HAIC effectively prevented recurrence. In several randomized studies, other investigators have reported that HAIC after resection of liver metastases prevented liver recurrences and improved patient outcome (16-18). Based on these reports, we can state that HAIC administered after local resection of tumor in Dukes C colorectal cancer patients had a prophylactic effect on hepatic metastases.

As is shown in **Table 3**, the effect of HAIC against extrahepatic metastases was limited. The total incidence of recurrence was almost the same in the two groups (25.7% *vs.* 30.6%) because of the increase of lung metastases in the HAIC group. This suggests the low systemic drug concentration produced during HAI would have little or no therapeutic effect on extrahepatic metastases. Thus, a combination of systemic and regional regimen is necessary for the effect of adjuvant chemotherapy to include other sites as well as the liver.

In conclusion, HAIC is an effective procedure for preventing metachronous liver metastasis and improving the prognosis in cases of advanced colorectal cancer, and this protocol we used in this pilot study can be safely employed in a prospective randomized study.

ACKNOWLEDGEMENTS

This research was supported in part by a Grant-in-Aid for Scientific Research (10671205) from the Ministry of Education, Science, Sports and Culture of Japan.

REFERENCES

1 **Cedermark BJ, Schultz SS, Bakshi S, Prthasarathy KL, Mittelman A, Evans JT:** The value of liver scan in the follow-up study of patients with adenocarcinoma of the colon and rectum. Surg Gynecol Obstet 1977; 144:745-748.
2 **Adson MA:** The resection of hepatic metastases. Another view. Arch Surg 1989; 124:1023-1024.
3 **Cruz P, McDonald GD, Cole HW:** Prophylactic treatment of cancer. Surgery 1956; 40:291-296.
4 **Morales F, Bell M, McDonald GD, Cole HW:** The prophylactic treatment of cancer at the time of operation. Ann Surg 1957; 146:588.
5 **Rougier P, Sahmoud T, Nitti D, Curran D, Docci R, Waele BD:** Adjuvant portal-vein infusion of fluorouracil and heparin in colorectal cancer: a randomised trial. European Organisation for Research and Treatment of Cancer, Gastrointestinal Tract Cancer Cooperative Group, the Gruppo Interdisciplinare Valutazione Interventi in Oncologia, and the Japanese Foundation for Cancer Research. Lancet 1998; 351:1677-1681.
6 **Gastrointestinal Tumor Study Group:** Adjuvant therapy of colon cancer - results of a prospectively randomized trial. N Engl J Med 1984; 310:737-743.
7 **Lawrence W Jr, Terz JJ, Horsley S 3d, Donaldson M, Lovett WL, Brown PW:** Chemotherapy as an adjuvant to surgery for colorectal cancer. Ann Surg 1975; 181:616-623.
8 **Higgins GA:** Adjuvant therapy for carcinoma of the colon and rectum. Int Adv Surg Oncol 1984; 7:77-111.
9 **Chen HS, Gross JF:** Intra-arterial infusion of anticancer drugs: theoretic aspects of drug delivery and review of responses. Cancer Treat Rep 1980; 64:31-40.
10 **Kemeny N, Niedzwiecki D, Shurgot B, Oderman P:** Prognostic variables in patients with hepatic metastases from colorectal cancer. Importance of medical assessment of liver involvement. Cancer 1989; 63:742-747.
11 **Ensminger WD, Gyves JW:** Clinical pharmacology of hepatic arterial chemotherapy. Semin Oncol 1983; 10:176-182.
12 **Izumi B, Tashiro S, Miyauchi Y:** Anticancer effects of local administration of mitomycin C via the hepatic artery or portal vein on implantation and growth of VX2 cancer injected into rabbit liver. Cancer Res 1986; 46:4167-4170.
13 **Ridge JA, Bading JR, Gelbard AS, Benua RS, Daly JM:** Perfusion of colorectal hepatic metastases. Relative distribution of flow from the hepatic artery and portal vein. Cancer 1987; 59:1547-1553.
14 **Daly JM, Kemeny N, Sigurdson E, Oderman P, Thom A:** Regional infusion for colorectal hepatic metastases. A randomized trial comparing the hepatic artery with the portal vein. Arch Surg 1987; 122:1273-1277
15 **Arai Y, Inabe Y, Takeuchi Y, Ariyoshi Y:** Intermittent hepatic arterial infusion of high-dose 5FU on a weekly schedule for liver metastases from colorectal cancer. Cancer Chemother Pharmacol 1997; 40:526-530.
16 **Kemeny N, Huang Y, Cohen AM:** Hepatic arterial infusion of chemotherapy after resection of hepatic metastases from colorectal cancer. N Engl J Med 1999; 341(27):2039-2048.
17 **Curley SA, Roh MS, Chase JL:** Adjuvant hepatic arterial infusion chemotherapy after curative resection of colorectal liver metastases. Am J Surg 1993; 166(6):743-746.
18 **Lorenz M, Staib-Sebler E, Koch B:** The value of postoperative hepatic arterial infusion following curative liver resection. Anticancer Res 1997; 17:3825-3833.

Application of RT-PCR to clinical diagnosis of micrometastasis of colorectal cancer: A translational research study*

OSAMU TAKAYAMA[1], HIROFUMI YAMAMOTO[1], KIMIMASA IKEDA[2], HIDEYUKI ISHIDA[3], TAKESHI KATO[4], MASAKI OKUYAMA[2], TOSHIYUKI KANOU[5], MUTSUMI FUKUNAGA[6], SHUSEI TOMINAGA[7], SHUNJI MORITA[8], YUJIRO FUJIE[1], HIROKI FUKUNAGA[1], MASAKAZU IKENAGA[1], MASATAKA IKEDA[1], MASAYUKI OHUE[1], MITSUGU SEKIMOTO[1], NOBUTERU KIKKAWA[4] and MORITO MONDEN[1]

[1]Department of Surgery and Clinical Oncology, Graduate School of Medicine, Osaka University; [2]Department of Surgery, Toyonaka Municipal Hospital; [3]Department of Surgery, Sakai Municipal Hospital; [4]Department of Surgery, Minoh City Hospital; [5]Department of Surgery, NTT West Osaka Hospital, Osaka; [6]Department of Surgery, Kansai Rosai Hospital, Hyogo; [7]Department of Surgery, Ikeda Municipal Hospital; [8]Department of Surgery, Yao Municipal Hospital, Osaka, Japan

Received February 2, 2004; Accepted April 16, 2004

Abstract. We previously reported in a retrospective study that CEA-based RT-PCR was useful for predicting the prognosis of patients with node-negative colorectal cancer. RT-PCR is well established for laboratory use, but many issues remain to be resolved prior to its clinical application. In addition to the false positive rate of RT-PCR, we addressed several issues, including the timing of lymph node sampling, stability of RNA after surgery, and reproducibility of results. After appropriate modification, including development of a tissue sampling kit, a multi-institutional clinical study was commenced prospectively from November 2001, and 100 patients were enrolled for examination of micrometastasis. RNA was stable in lymph nodes for up to 3 h after surgical resection. This range of sampling time was acceptable to the surgeons. RNA was well preserved in RNA later™ at -20°C for 3 weeks. Dilutions of MKN45 and LoVo cells served as positive controls for conventional PCR since these controls were found to be highly stable and ensured reproducibility. Moreover, simultaneous use of quantitative PCR (Light Cycler™) ensured double confirmation of the results. Our clinical study showed that the quality of RNA was excellent or good in most samples (98 of 100; 98%). Twenty-four of 98 (24.5%) cases were judged to be micrometastasis-positive. In conclusion, the current translational research study established a clinically feasible RT-PCR system for micrometastasis. Our system could potentially be useful as a clinical tool.

Correspondence to: Dr Hirofumi Yamamoto, Department of Surgery and Clinical Oncology, Graduate School of Medicine, Osaka University, 2-2 Yamadaoka, Suita City, Osaka 565-0871, Japan
E-mail: kobunyam@surg2.med.osaka-u.ac.jp

*Multicenter Clinical Study Group of Osaka, Colorectal Cancer Division

Abbreviations: cDNA, complementary DNA; CEA, carcinoembryonic antigen; CK20, cytokeratin 20; CRC, colorectal cancer; LN, lymph node; PBGD, porphobilinogen deaminase; RT-PCR, reverse transcriptase-polymerase chain reaction

Key words: colorectal cancer, micrometastasis, carcinoembryonic antigen, real-time PCR, translational research

Introduction

Reverse transcriptase-polymerase chain reaction (RT-PCR) is a powerful method for detection of micrometastases of colon cancer cells. It has been reported that 29.6-100% of node-negative (N0) patients with colorectal cancer (CRC) had micrometastasis in lymph nodes (LN) by RT-PCR (1-6). Liefers *et al* showed that carcinoembryonic antigen (CEA)-based RT-PCR-positive cases had a significantly poorer prognosis than RT-PCR-negative cases in a series of 26 stage II CRCs (1). We previously showed that RT-PCR using CEA or cytokeratin 20 (CK20) as a genetic marker was helpful to predict the rapid recurrence of CRC patients (2). Moreover, our retrospective study using paraffin blocks showed that CEA-based RT-PCR-positive stage II CRCs had a significantly poorer prognosis than CEA RT-PCR-negative CRCs during more than 5 years of follow-up (3). These findings suggest that RT-PCR may be a useful tool to predict clinical outcome and help in selecting appropriate treatment for node-negative CRC patients.

At present, CEA-based RT-PCR is well established for laboratory use, but much remains to be resolved prior to its practical application to clinical use. Firstly, false positivity has been a fundamental problem associated with the PCR technique. This issue was avoidable by establishment of PCR

conditions with reasonable sensitivity, as described in our earlier studies (2,3). Thus, amplification of PCR for CEA transcript was restricted to 35 cycles by the appearance of a few false positive samples in normal control LNs.

Secondly, the stability of RNA in LN must be assessed. Surgeons usually collect LNs from resected specimens several hours after surgery. It is probable that RNA might be impaired during this period since RNA from certain tissues undergoes degradation very quickly. This is a critical issue because if degradation of RNA in LN occurs extremely rapidly, diagnosis of micrometastasis by RT-PCR is practically impossible in most hospitals. Moreover, in cost-benefit terms, it would be better to perform RNA extraction and RT-PCR solely in node-negative CRC patients, not in node-positive patients. For this purpose, RNA in LNs must be well preserved until the pathological report is available, which usually takes about 1-2 weeks.

Thirdly, particular attention has to be taken to avoid contamination of tumor cells during LN sampling procedures. Elimination of RNase in the environment is also a strict requirement (7). However, it would be a practical difficulty at most hospitals to prepare tools specialized for such a purpose, for example, RNase-free forceps, scissors and blades. Therefore, certain strategies are necessary to facilitate this procedure. In addition, to establish molecular detection using RNA sampling as a generally applicable technique, demonstration of LN sampling for educational purposes is also important during the first sampling opportunities.

Finally, the greatest hurdle to overcome with the RT-PCR method is reproducibility, especially when very minimal transcript is present (1,8). This difficult problem must be absolutely resolved because clinical treatment could differ solely on the basis of positive or negative results of RT-PCR.

As described above, many issues remain to be resolved before RT-PCR can be clinically applied for the diagnosis of micrometastasis. Here, to advance our basic research (2,3) toward a clinical stage, we conducted a translational research study and established a micrometastasis detection system using RT-PCR that can be applied for clinical use.

Materials and methods

Hospital groups. The clinical study was performed with the collaboration of the Department of Surgery and Clinical Oncology, Graduate School of Medicine, Osaka University, and its related hospitals (n=17) from November 2001 to February 2003. The list of participating hospitals and co-operative physicians is shown in the Appendix. To obtain LN samples from CRC patients, the project was approved by the ethics committee at each hospital, and informed consent was obtained from the patients.

Surgical specimens. Within 3 h of surgical resection, all lymph nodes were collected, cut into halves using the disposable tissue sampling kit without cross-contamination from the main CRC tumor. Half of each node was fixed in 10% buffered formalin and embedded in paraffin for routine histopathological examination. The other half was preserved in a tube containing RNA later (Ambion, Austin, TX) (10-12) at -20°C until RNA extraction.

RNA extraction. Tissue specimens were minced with a disposable homogenizer (IEDA™, Tokyo, Japan) in TRIzol Reagent (Invitrogen, Carlsbad, CA). RNA extraction was performed as described previously (2,9). Purified RNA was quantified and assessed for purity by UV spectrophotometry. For assessment of RNA quality, 1 μg of RNA from each LN was electrophoresed on a 0.8% agarose mini-gel and ribosomal RNAs and the extent of degradation was visualized with ethidium bromide.

Conventional RT-PCR. Conventional RT-PCR was performed as described previously (2,3). Briefly, complementary DNA (cDNA) was generated using avian myeloblastosis virus reverse transcriptase using the procedure provided by the supplier (Promega, Madison, WI). Reverse transcription was performed at 42°C for 60 min, followed by heating at 95°C for 10 min. The primer sequences for PCR amplification of CEA (2,3) and porphobilinogen deaminase (PBGD) (13,14) were as follows: CEA (forward), 5'-TCTGGAACTTCTCCT GGTCTCTCAGCTGG; and CEA (reverse), 5'-TGTAGCTG TTGCAAATGCTTTAAGGAAGAAGC. PBGD (forward), 5'-TGTCTGGTAACGGCAATGCGGCTGCAAC; and PBGD (reverse), 5'-TCAATGTTGCCACCACACTGTCCG TCT. The size of amplicons for CEA and PBGD was 160 and 120 bp, respectively.

PCR was performed with a GenAmp® PCR System 9600 (Perkin-Elmer Cetus, Foster City, CA). PCR amplification was performed in a 25-μl reaction mixture containing 2 μl of cDNA, 1X PCR buffer, 1.5 mM $MgCl_2$, 0.8 mM deoxynucleotide triphosphatase, 0.2 μM each primer and 1 unit of Taq DNA polymerase (AmpliTaq Gold; Roche Molecular Systems, Pleasanton, CA). PCR conditions were set as follows: a) for CEA; one cycle of denaturing at 95°C for 12 min, followed by 35 cycles at 95°C for 1 min and 72°C for 1.5 min before a final extension at 72°C for 10 min, and b) for PBGD; one cycle of denaturing at 95°C for 12 min, followed by 40 cycles at 95°C for 1 min, 62°C for 1 min and 72°C for 1.5 min before a final extension at 72°C for 10 min. The reaction mixture (10 μl) was electrophoresed on a 2% agarose gel and visualized with ethidium bromide.

Cell lines and cell culture conditions. The human gastric cancer cell line MKN45 was obtained from Health Science Research Resources Bank (Tokyo, Japan) (15). The LoVo, HT29 and DLD1 human colon carcinoma cell lines were obtained from the American Type Culture Collection (16). They were grown in Dulbecco's modified Eagle's medium plus 10% fetal bovine serum, 100 units/ml penicillin and 100 μg/ml streptomycin, in 5% CO_2 at 37°C.

Cell production of control panel using CEA-expressing cells. RNA (1 μg) from four different cancer cell lines (MKN45, LoVo, HT29, and DLD1) was subjected to RT reaction. Each cDNA was mixed with cDNA prepared from rat spleen to make 10-fold serial dilutions of $1x10^{-1}$ to $1x10^{-5}$. PCR was performed using CEA primers and PBGD primers.

Quantitative PCR assay with Light Cycler. Fluorescence PCR was performed using the Light Cycler (Roche Diagnostics, Mannheim, Germany) in a 10-μl PCR reaction containing

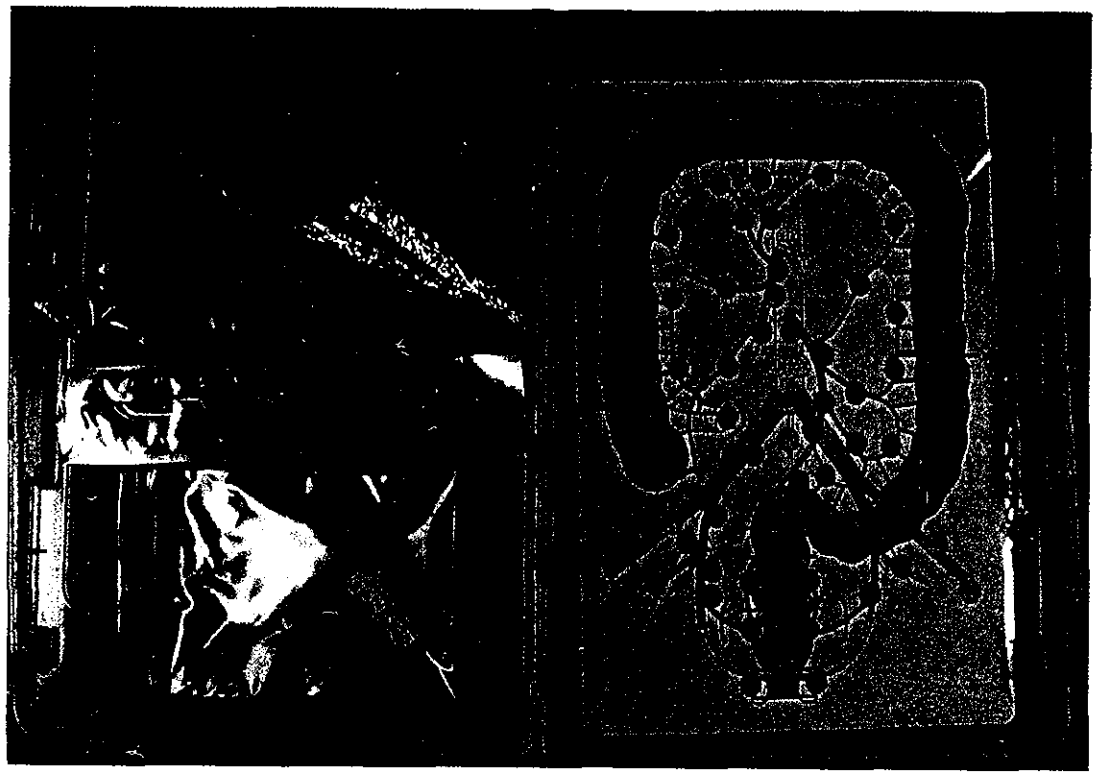

Figure 1. Tissue sampling kit. The kit contained a set of scissors, forceps, scalpel, a tube containing special liquid for RNA preservation (RNA later) and a board for arrangement of LNs. The kit was pre-treated with RNase-away to eliminate RNase activity.

0.2 μM of each primer, 1x Light Cycler-Fast start DNA Master SYBR Green I (Roche Diagnostics), 4 mM $MgCl_2$, and 2 μl of cDNA as template. PCR conditions were as follows: one cycle of denaturing at 95°C for 10 min, followed by 40 cycles at 95°C for 15 sec, 62°C for 10 sec and 72°C for 18 sec. Fluorescence was acquired at the end of each 72°C extension phase. The melting curves of final PCR products were analyzed after 40 cycles of PCR amplification by cooling the samples to 65°C, increasing the temperature up to 99°C at a rate of 0.1°C/sec, and monitoring fluorescence at each 0.1°C. Quantification data were analyzed using Light Cycler analysis software (Roche Diagnostics GmbH) as recommended by the manufacturer. The standard curves for quantification of CEA or PBGD mRNAs were drawn using 10-fold dilutions of cDNA from MKN45 cells. The sequences of CEA and PBGD primers were the same as those used in the conventional PCR.

Results

Tissue sampling kit. To avoid contamination of cancer cells, a disposable tissue sampling kit was developed (Fig. 1). The box was 30.0x23.0x3.8 cm in size, containing a set of scissors, forceps, blade, a tube containing special liquid for RNA preservation (RNA later) and a board for arrangement of LNs. RNA later can be stored at room temperature. The box and all tools were rendered RNase-free by pretreatment with RNase away (Molecular BioProducts, inc., San Diego, CA).

Inquiry to related hospitals about sampling practices. We asked surgeons working at related hospitals (n=17) about the time they usually collect LNs from the resected specimens after surgery. As shown in Table I, LN sampling was performed within 3 h after surgery in most hospitals (17 of 18 hospitals including our institute).

Table I. When do surgeons collect lymph nodes after surgery?

Hours	Hospitals
<1	6
<2	9
<3	2
<24	1
Total	18

Stability of RNA in LNs. LNs from 7 CRC patients were left at room temperature for 1, 2 and 3 h after surgery, at which times RNA was extracted. RNA quality was assessed by electrophoresis. Ribosomal RNAs at 28S and 18S were quite well preserved even after 3 h in all LN samples tested (Fig. 2A), while RNA extracted from tumor tissues was preserved at good quality at 3 h in 5 of 7 cases (data not shown). We then examined how long RNA in LNs could be preserved when LNs were stored in RNA later at -20°C. As shown in Fig. 2B, RNA was of good quality even after 3 weeks of storage.

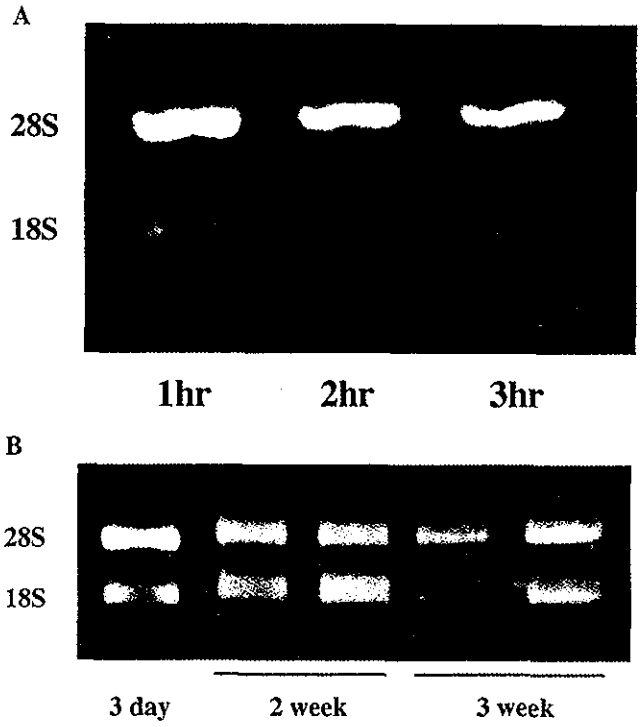

Figure 2. Stability of RNA in LNs. (A), Assessment of timing of LN sampling. LNs were left at room temperature for 1, 2 and 3 h after surgery and then RNA was extracted. Prominent doublet bands of 28S and 18S ribosomal RNAs were well preserved even in the 3-h samples. RNA extracts from a representative CRC patient are shown here. (B), Assessment of LN storage. LNs were collected from the same CRC patient. They were stored in RNA later at -20°C for 3 days, 2 weeks and 3 weeks and then RNA was extracted. RNA quality was sufficient even after 3 weeks of storage.

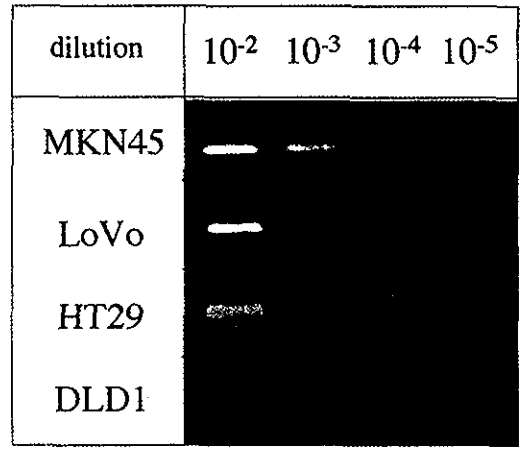

Figure 3. Control panel using CEA-expressing cells. A control panel was constructed as positive controls for conventional PCR. Using CEA mRNA as a marker, RT-PCR yielded bands for dilutions of MKN45, LoVo, HT29, but not DLD1 cells. MKN45 and LoVo cells exhibited good reproducibility.

Control panel using CEA-expressing cells. A control panel was constructed as positive control for conventional PCR. Using CEA mRNA as a marker, PCR yielded bands for dilutions of MKN45, LoVo, HT29, but not DLD1 cells (Fig. 3). Experiments were repeated 22 times using the LoVo cells at dilutions of 10^{-2}-10^{-4}, and the MKN45 cells at dilutions of 10^{-2}-10^{-5}, including all steps, that is, from RNA extraction to reverse transcription to PCR, and reproducible results were obtained 19 times. In one repetition, the highest dilutions (MKN45 at dilution of 10^{-5}, LoVo at dilution of 10^{-4}) yielded visible bands that should not have emerged. In the remaining two repetitions, there were no visible bands at all dilutions, indicating simple technical error. The unusual patterns in these three experiments reverted to the typical pattern by a single repeat experiment, indicating that these control dilutions were highly stable and ensured reproducibility. On the other hand, HT29 cells showed unstable results. Thus, at the highest dilution (10^{-4}), a visible band appeared in 6 of 10 repeat experiments (data not shown).

Modification of real-time PCR for CEA mRNA measurement. To measure CEA mRNA levels, we modified a real-time PCR method previously reported by our laboratories (17). First, human peripheral lymphoid cells were used in the original study to prepare serial dilutions of MKN45 cells when the standard curves were drawn. However, human blood is not suitable as a diluent for clinical workup, so we instead used rat spleen as a diluent. cDNA from rat spleen was not amplified with the primers for human CEA gene expression (data not shown). Since we have noted that the RT reaction itself occasionally produces inter-experimental deviation (data not shown), cDNA derived from 1 μg RNA of MKN45, rather than the RNA itself, was serially diluted with cDNA of rat spleen in making standard curves (Fig. 4A). In 40 separate experiments, the modified system rendered the standard curves highly stable and reproducible within the range of $1.0x10^{-1}$ to $1.0x10^{-4}$ (Fig. 4B). The standard deviation was <10% in each dilution in this range, but the system did not assure the measurement value at a dilution of $1x10^{-5}$ (data not shown).

The Light Cycler provides another benefit in that the melting temperature indicates whether the PCR product is real or not. This utility is based on the finding that the melting temperature is determined by the content of individual PCR products. When the bands for CEA were very faint by conventional PCR, it was sometimes difficult to distinguish them from non-specific bands (Fig. 5). The melting temperature determined by the MKN45-positive control sample revealed that sample no. 1 expressed a real CEA band, whereas samples nos. 2-4 displayed non-specific bands because their melting temperature was significantly different from that of the positive control.

Multi-institution group study. Using the above system, we commenced a multi-institutional clinical study in November 2001 to assess the actual incidence of micrometastasis of stage II CRC. Paracolic LNs were collected within 3 h after surgery, stored in RNA later at -20°C, and then moved to our laboratory once a week in a dry ice package. Homogenized LNs were mixed and RNA was extracted. All samples were first examined for RNA quality, and classified into four levels according to degradation pattern of ribosomal RNAs at 28S and 18S by electrophoresis; A, Excellent (28S>18S, without degradation); B, Fairly good (28S≥18S, only partial degradation, if any); C, Poor (18S>28S, with large degradation); D, Unequivocal (no visible ribosomal RNA, all

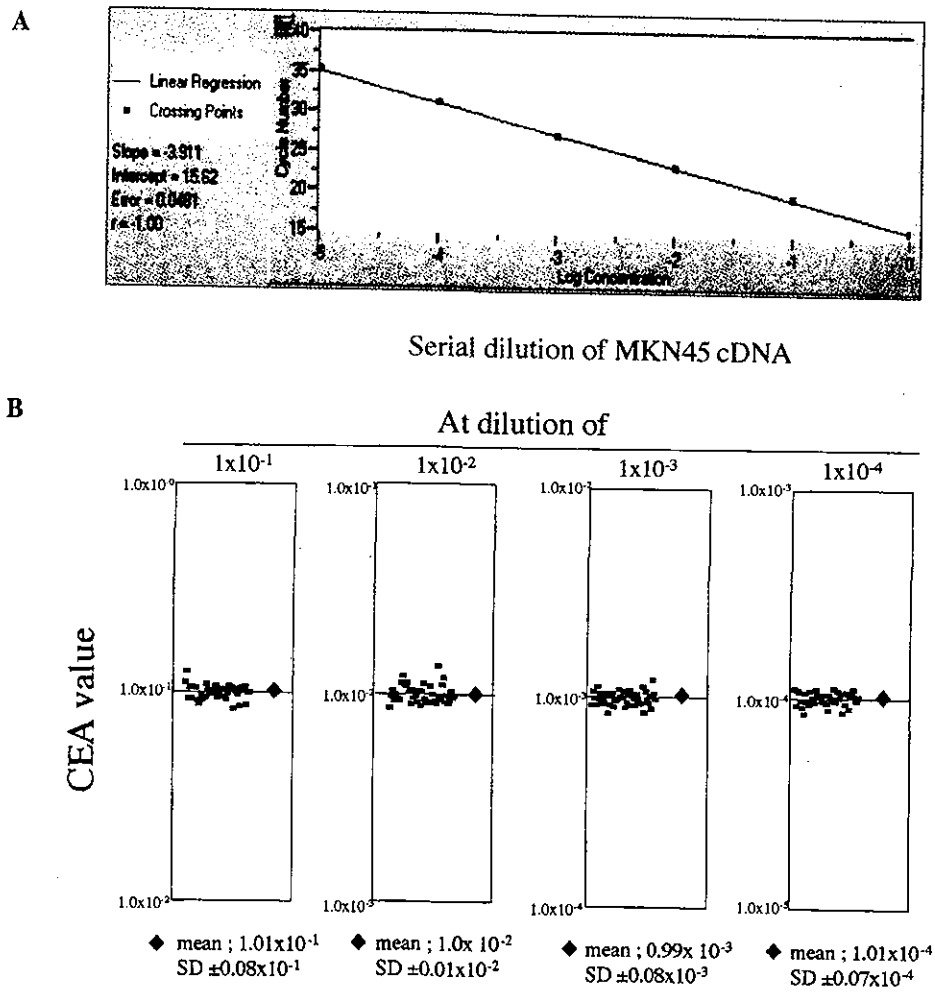

Figure 4. Real-time PCR for measurement of CEA mRNA. (A), Standard curve. cDNA derived from 1 μg RNA of MKN45 was serially diluted with cDNA of rat spleen at dilutions of 10^{0}-10^{-5}. Standard curves were drawn by plotting the PCR cycle number at which each diluted sample started making PCR product. (B), The modified RT-PCR system rendered the standard curves highly stable and reproducible within the range of $1.0x10^{-1}$ to $1.0x10^{-4}$. Standard deviation was <10% in each dilution within this range.

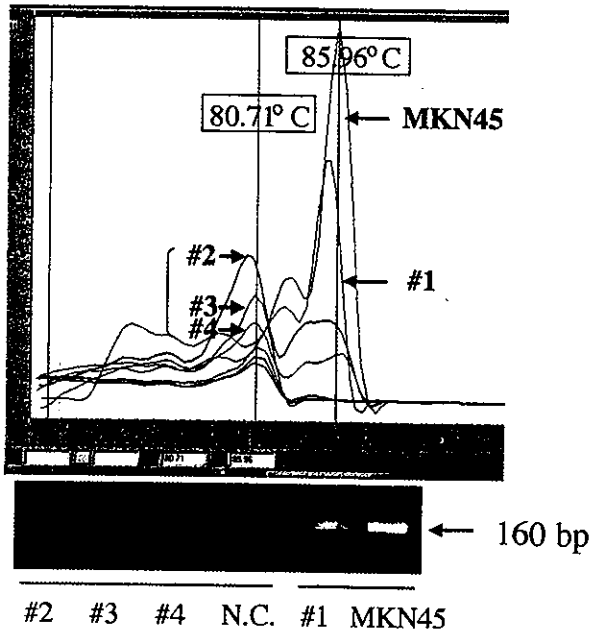

Figure 5. Melting temperature of the PCR product. The melting temperature determined by the MKN45-positive control sample was 85.9°C and sample no. 1 had a similar melting temperature, indicating that it expressed a real CEA band, whereas sample nos. 2-4 produced non-specific bands because their melting temperature was around 80.7°C. NC., negative control.

RNA degraded) (Fig. 6). Most of the samples (98 of 100 cases; 98%) were classified into levels A and B. Expression of the PBGD gene was evident in these samples (data not shown), and only samples of levels A and B were subject to further RT-PCR assay by both conventional PCR and modified real-time PCR. Fig. 7 shows two representative cases. Case 1 expressed a CEA band compatible with that of MKN45 dilution at 10^{-4} and yielded a CEA value of $1.9x10^{-4}$ by real-time PCR. Case 2 did not express the CEA band and the CEA value was $3.7x10^{-5}$, which was under the measurable range of $1.0x10^{-4}$ to $1.0x10^{-1}$. Analyses of a total of 98 CRC cases indicated that they were successfully divided into two groups, band-positive with a high quantity of CEA (24 of 98 cases: 24.5%) and band-negative with a low quantity of CEA (74 of 98: 75.5%) (Fig. 8). Only one case with ambiguous faint bands were judged as negative by analysis of melting temperature (data not shown).

Discussion

Even among node-negative CRC patients, approximately 10-20% suffer from relapse within 5 years (18). Since the majority of stage II CRCs are thought to still be localized and not yet systemic disease, there is a debate about appropriate

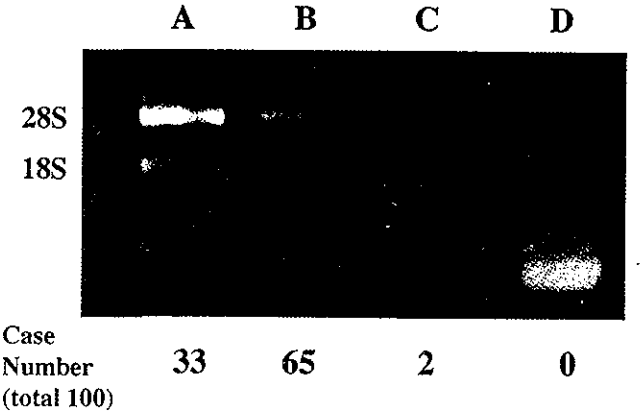

Figure 6. Assessment of RNA quality in clinical samples. According to the degradation pattern of ribosomal RNAs, clinical samples were classified as follows; (A), Excellent (28S>18S, without degradation); (B), Fairly good (28S≥18S, only partial degradation, if any); (C), Poor (18S>28S, with large degradation); (D), Unequivocal (no visible ribosomal RNA, all RNA degraded). Ninety-eight of 100 (98%) cases were classified into levels A and B.

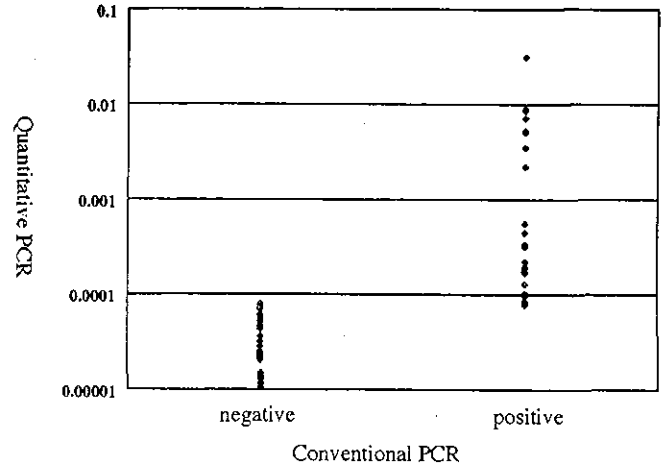

Figure 8. Analyses of a total of 100 CRC cases for micrometastasis. The patients were divided into two groups: i) band-positive with a high CEA quantity (24 of 98 cases: 24.5%) and ii) band-negative with a low CEA quantity (74 of 98: 75.5%).

post-operative chemotherapy for stage II CRC patients. Indeed, among our related hospital groups, more than half (12 of 18; 67%) presently use no post-operative chemotherapy, whereas the other 6 hospitals often use 5-FU-based chemotherapy for this group. Since there are no clear indicators whether or not to treat, it is therefore important to discriminate those at high risk for disease recurrence among stage II CRCs. For this purpose, we found that although information on clinical and pathological parameters was not helpful, our retrospective study showed that CEA-based RT-PCR was useful (3).

This finding was exciting, yet we should be cautious as we cannot exclude the possibility that LNs collected in the past might have been subject to contamination of cancer cells via scissors or blades used for tumor excision. Therefore, a prospective study using a strict sampling procedure was essential, ideally including a larger number of CRCs, to confirm the previous results. However, as mentioned in Introduction, many issues remain regarding the use of RT-PCR for clinical diagnosis. Osaka University Hospital is well supplied with surgeons and medical staff, and collection of LNs is usually completed in less than 1 h of excision. On the other hand, there are only a limited number of surgeons at related hospitals and often it is not feasible to collect LNs within 1 h. If the RNA in LNs was easily degraded, it would be a major technical problem for establishing RT-PCR for general use to detect micrometastasis. Fortunately, we determined the optimal LN sampling time to be within 3 h after resection, a time frame feasibly met by surgeons and during which the quality of RNA was well preserved (Table I, Fig. 2A). This result regarding the preservation time of RNA in LNs was far better than had been anticipated, which was encouraging as it indicates that RT-PCR assay for CEA mRNA in LNs could be practically applicable in most general hospitals. Moreover, LNs could be stored for at least 3 weeks (Fig. 2B), if stored in RNA later at -20°C. Storage

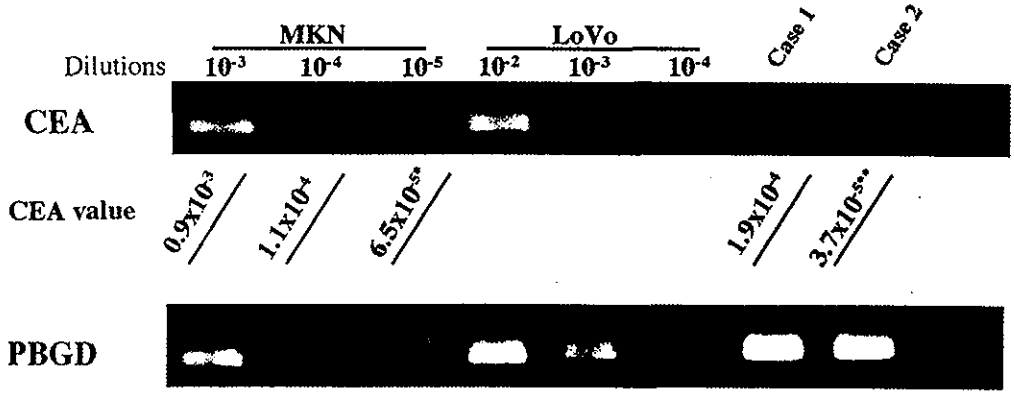

Figure 7. Two representative cases in the prospective study. Case 1 expressed a CEA band compatible with that of the MKN45 dilution at 10^{-4} and gave a CEA value of 1.9×10^{-4} by real-time PCR. Case 2 did not express a CEA band and the CEA value was 3.7×10^{-5}, which was under the measurable range of 1.0×10^{-4} to 1.0×10^{-1}. Both samples expressed intense bands for the housekeeping PBGD gene. *,**These CEA values were outside the measurable range.

at -80°C is not necessarily required. This result is convenient on a cost-benefit basis as it means that the RT-PCR assay could be applied solely to node-negative CRC patients after pathological analysis.

When RNA is utilized as the material for examination, special attention must be taken to avoid contamination by RNase in the LN sampling procedure. To address this issue we developed a tissue sampling kit. This kit was intended for busy surgeons working at related hospitals to facilitate LN sampling. When we first explained the method of LN sampling for RT-PCR to surgeons, the majority insisted that they would not be able to prepare RNase-free equipment for each procedure. After introducing the tissue sampling kit, they agreed to participate in the project of molecular detection of micrometastasis. The kit contains a disposable blade, scissors and forceps that are rendered RNase-free. After one or two educational demonstrations of LN sampling (mainly executed by Osamu Takayama, one of the main investigators), surgeons at each hospital could execute appropriate LN sampling, so that artificial contamination of cancer cells over LNs could be avoided.

False positive reactions and lack of reproducibility are the two major concerns with regard to the PCR technique. With respect to false positivity, in our earlier studies we assessed optimal PCR conditions in which LNs from non-cancer patients would never be amplified (2,3). Our results from these studies indicated that we should perform a single PCR amplification of 35 cycles for the CEA transcript, at least in our PCR system.

Reproducibility is a problem that remains to be fully addressed. This issue is especially important in detection of the minimal level of mRNA expression. A single intense positive control is not useful as a control for such minimal transcripts because a slight decrease in PCR efficiency could easily produce false negative results even with preservation of the intense control signal. To address this issue, we have constructed a control panel using CEA-expressing cells. Cancer cell lines express different levels of CEA mRNA and we tried to find dilutions of appropriate cell lines that would show reproducible results under our PCR conditions. Although the HT29 and DLD1 cell lines were not appropriate for this purpose, MKN45 and LoVo cells exhibited high reproducibility. With a panel of dilutions of these two cell lines, our prospective clinical study proceeded and the expected expression pattern was obtained in almost all PCR reactions (data not shown).

We previously showed that amount of micrometastasis of CRC varied quite widely (17). In a prospective study, it is important to quantify micrometastasis so that a critical cut-off level for the prediction of prognosis can be determined. For this purpose we modified our real-time PCR method. As diluents of MKN45 cells, we first used *E. coli*, but this was not feasible as the primers for the human CEA sequence unexpectedly produced PCR products from cDNA derived from *E. coli* (data not shown). We then employed rat spleen since it was used to measure PBGD mRNA in our previous study (17) and found that it was also appropriate for measuring CEA mRNA. Certain DNA plasmids may alternatively be applicable as diluents. The modified system can measure CEA transcripts accurately within the range of $1x10^{-1}$ to $1x10^{-4}$. The minimal detectable CEA band of MKN45 cells (at dilution of 10^{-4}) coincidentally corresponded to a CEA value of approximately $1.0x10^{-4}$ (Fig. 7), and thus, double confirmation was possible.

In this study, we performed a translational research analysis and established a clinically feasible RT-PCR system. To date, using this system, more than 98 stage II CRCs have been prospectively examined for micrometastasis. The percentage of band-positive cases (24.5%) was somewhat lower than that (29.6%) reported in our retrospective study (3). This could be due to differences in sampling procedures between the retrospective and prospective studies. The strict sampling procedure using the tissue sampling kit in our current study would not permit artificial contamination of cancer cells, whereas such contamination was likely in the retrospective study. The present study also indicates that RT-PCR for micrometastasis is applicable not only at specified institutes, but also at general hospitals. Therefore, it may become a powerful clinical tool, if our prospective study confirms that RT-PCR for micrometastasis is useful for predicting the prognosis of stage II CRC.

Acknowledgments

This work was supported by a Grant-in-Aid for Cancer Research from the Ministry of Education, Science, Sports, and Culture Technology, Japan, to H.Y.

References

1. Liefers GJ, Cleton-Jansen AM, van de Velde CJ, Hermans J, van Krieken JH, Cornelisse CJ and Tollenaar RA: Micrometastases and survival in stage II colorectal cancer. N Engl J Med 339: 223-228, 1998.
2. Miyake Y, Yamamoto H, Fujiwara Y, *et al*: Extensive micrometastases to lymph nodes as a marker for rapid recurrence of colorectal cancer: a study of lymphatic mapping. Clin Cancer Res 7: 1350-1357, 2001.
3. Noura S, Yamamoto H, Ohnishi T, *et al*: Comparative detection of lymph node micrometastases of stage II colorectal cancer by reverse transcriptase polymerase chain reaction and immunohistochemistry. J Clin Oncol 20: 4232-4241, 2002.
4. Weitz J, Kienle P, Magener A, *et al*: Detection of disseminated colorectal cancer cells in lymph nodes, blood and bone marrow. Clin Cancer Res 5: 1830-1836, 1999.
5. Futamura M, Takagi Y, Koumura H, Kida H, Tanemura H, Shimokawa K and Saji S: Spread of colorectal cancer micrometastases in regional lymph nodes by reverse transcriptase-polymerase chain reactions for carcinoembryonic antigen and cytokeratin 20. J Surg Oncol 68: 34-40, 1998.
6. Rosenberg R, Hoos A, Mueller J, *et al*: Prognostic significance of cytokeratin-20 reverse transcriptase polymerase chain reaction in lymph nodes of node-negative colorectal cancer patients. J Clin Oncol 20: 1049-1055, 2002.
7. Sambrook J and Russel DW: Molecular Cloning. A Laboratory Manual. 3rd edition. Cold Spring Harbor Laboratory Press, New York, 2001.
8. Van Trappen PO, Gyselman VG, Lowe DG, *et al*: Molecular quantification and mapping of lymph-node micrometastases in cervical cancer. Lancet 357: 15-20, 2001.
9. Chomczynski P and Sacchi N: Single-step method of RNA isolation by acid guanidinium thiocyanate-phenol-chloroform extraction. Anal Biochem 162: 156-159, 1987.
10. Florell SR, Coffin CM, Holden JA, *et al*: Preservation of RNA for functional genomic studies: a multidisciplinary tumor bank protocol. Mod Pathol 14: 116-128, 2001.
11. Rodrigo MC, Martin DS, Redetzke RA and Eyster KM: A method for the extraction of high-quality RNA and protein from single small samples of arteries and veins preserved in RNAlater. J Pharmacol Toxicol Methods 47: 87-92, 2002.

12. Grotzer MA, Patti R, Geoerger B, Eggert A, Chou TT and Phillips PC: Biological stability of RNA isolated from RNAlater-treated brain tumor and neuroblastoma xenografts. Med Pediatr Oncol 34: 438-442, 2000.
13. Nagel S, Schmidt M, Thiede C, Huhn D and Neubauer A: Quantification of Bcr-Abl transcripts in chronic myelogenous leukemia (CML) using standardized, internally controlled, competitive differential PCR (CD-PCR). Nucleic Acids Res 24: 4102-4103, 1996.
14. Takemasa I, Yamamoto H, Sekimoto M, *et al*: Overexpression of CDC25B phosphatase as a novel marker of poor prognosis of human colorectal carcinoma. Cancer Res 60: 3043-3050, 2000.
15. Kaneko K, Yano M, Yamano T, *et al*: Detection of peritoneal micrometastases of gastric carcinoma with green fluorescent protein and carcinoembryonic antigen promoter. Cancer Res 61: 5570-5574, 2001.
16. Lengauer C, Kinzler KW and Vogelstein B: DNA methylation and genetic instability in colorectal cancer cells. Proc Natl Acad Sci USA 94: 2545-2550, 1997.
17. Miyake Y, Fujiwara Y, Ohue M, *et al*: Quantification of micrometastases in lymph nodes of colorectal cancer using real-time fluorescence polymerase chain reaction. Int J Oncol 16: 289-293, 2000.
18. Ratto C, Sofo L, Ippoliti M, Merico M, Doglietto GB and Crucitti F: Prognostic factors in colorectal cancer. Literature review for clinical application. Dis Colon Rectum 41: 1033-1049, 1998.

Appendix

Participants in clinical study: K. Ikeda, M. Okuyama, T. Shimano: Department of Surgery, Toyonaka Municipal Hospital, Osaka; T. Kato, M. Tsujie, N. Kikkawa: Department of Surgery, Minoh City Hospital, Osaka; M. Fukunaga, N. Tomita: Department of Surgery, Kansai Rosai Hospital, Hyogo; H. Ishida, H. Furukawa: Department of Surgery, Sakai Municipal Hospital, Osaka; T. Kanou, S. Ohnishi, T. Monden: Department of Surgery, NTT West Osaka Hospital, Osaka; S. Tominaga, T. Kobayashi: Department of Surgery, Ikeda Municipal Hospital, Osaka; S. Morita, N. Shibata: Department of Surgery, Yao Municipal Hospital, Osaka; N. Tanaka, H. Maruyama: Department of Surgery, Kawanishi City Hospital, Hyogo; K. Murata, M. Kameyama: Department of Surgery, Osaka Medical Center for Cancer and Cardiovascular Diseases, Osaka; H. Ohta, K. Yamasaki: Department of Surgery, Saiseikai Senri Hospital, Osaka; Y. Uemura, K. Kobayashi: Department of Surgery, Kinki Central Hospital of the Mutual Aid Association of Public School Teachers, Hyogo; M. Amano, S. Ohshima: Department of Surgery, Nishinomiya Municipal Central Hospital, Hyogo; M. Watase, Y. Ogawa: Department of Surgery, Tane General Hospital, Osaka; F. Kimura, M. Yamamoto: Department of Surgery, Itami City Hospital, Hyogo; K. Fukuda, H. Hatanaka: Department of Surgery, Fujimoto Hospital, Osaka; Y. Watanabe, T. Kabuto: Department of Surgery, Osaka Seamen's Insurance Hospital, Osaka; N. Yamamoto, H. Oka: Department of Surgery, Moriguti Keijinnkai Hospital, Osaka, Japan.

Hepatic Expression of *ANG2* RNA in Metastatic Colorectal Cancer

Minoru Ogawa,[1] Hirofumi Yamamoto,[1] Hiroaki Nagano,[1] Yasuhiro Miyake,[1] Yurika Sugita,[1] Taishi Hata,[1] Byung-no Kim,[1] Chew Yee Ngan,[1] Bazarragchaa Damdinsuren,[1] Masakazu Ikenaga,[1] Masataka Ikeda,[1] Masayuki Ohue,[1] Shoji Nakamori,[1] Mitsugu Sekimoto,[1] Masato Sakon,[1] Nariaki Matsuura,[2] and Morito Monden[1]

We examined the RNA content of the gene encoding angiopoietin (Ang)-2, a modifier of angiogenesis, in hepatic metastases of colorectal cancer (CRC) to explore the role of this protein in neovascularization of metastatic foci. Metastatic CRC exhibited notable blood flow and tumor vessel formation at tumor frontiers. Reverse-transcription polymerase chain reaction assays indicated that the *ANG2* RNA content was greater in metastatic CRC than in primary CRC. Investigation of metastatic foci using laser capture microdissection revealed that the RNA content of *ANG2*, but not *ANG1*, increased from the bordering liver region to the periphery of the metastatic disease, and also from the periphery to the intermediate portion of the metastatic lesion; immunohistochemical analysis confirmed that there was a corresponding gradual increase in Ang-2 protein expression. Tie-2, a receptor for angiopoietins, was preferentially expressed in the bordering liver region rather than in metastatic CRC. Vascular endothelial growth factor (VEGF) also exhibited an expression pattern similar to that of Ang-2, and there was a significant correlation between the RNA content of *ANG2* and that of *VEGF* in dissected samples ($P = .002$). Western blot analysis suggested that expression of Ang-1, Ang-2, Tie-2, and VEGF may be regulated at a transcriptional level. The increase in *ANG2* RNA content from the peripheral portion of the tumor to the intermediate portion, coinciding with the decrease in recruitment of periendothelial supporting cells around the vascular endothelial cells, suggests that Ang-2 may play a role in the immaturity of tumor vessels. In conclusion, the current study suggests that Ang-2 and VEGF may cooperate to enhance the formation of new blood vessels in metastases of CRC to the liver. (HEPATOLOGY 2004;39:528–539.)

Colorectal cancer (CRC) is a common malignancy worldwide. Although 84%–92% of patients with CRC are treated with surgical resection, more than half of these patients subsequently develop disease recurrence,[1] the most common type of recurrence being CRC metastatic to the liver, which often is associated with mortality.[2,3] Metastasis of CRC to the liver is a complex multistep process, which includes adherence of metastatic cells to endothelial cells (ECs), invasion across the endothelial basement membrane, cell proliferation, and neovascularization.[4] It was reported that tumor vessels appeared in human liver metastases when metastatic foci grew to 200 μm in diameter and that the density of tumor vessels increased as tumor size increased.[5] Angiogenesis is essential for tumor growth and expansion, because the resulting blood vessels supply malignant cells with sufficient oxygen and nutrition.[6,7] Therefore, interruption of this process is considered to be a strategy for preventing CRC metastases to the liver.

Recent studies have focused on novel endothelial growth factors such as angiopoietins (Ang), which are ligands for the endothelium-specific tyrosine kinase receptor Tie-2.[8–10] Ang molecules play crucial roles in normal vascular development and in embryonic angio-

Abbreviations: CRC, colorectal cancer; EC, endothelial cell; Ang, angiopoietin; PESC, periendothelial supporting cell; RT-PCR, reverse-transcription polymerase chain reaction; LCM, laser capture microdissection; VEGF, vascular endothelial growth factor; SMA, smooth muscle actin.

From the [1]Department of Surgery and Clinical Oncology, Graduate School of Medicine, Osaka University, Osaka, Japan; and [2]Department of Pathology, School of Allied Health Science, Faculty of Medicine, Osaka University, Osaka, Japan.

Received March 27, 2003; accepted November 6, 2003.

Supported by a grant-in-aid from the Ministry of Education, Culture, Sports, Science, and Technology of Japan (to H.Y.).

M.O. and H.Y. contributed equally to this work.

Address reprint requests to: Hirofumi Yamamoto, M.D., Ph.D., Department of Surgery and Clinical Oncology, Graduate School of Medicine, Osaka University, 2-2 Yamada-oka, Suita-City, Osaka 565-0871, Japan. E-mail: kobunyam@surg2.med.osaka-u.ac.jp; fax: +81-6-6879-3259

Published online in Wiley InterScience (www.interscience.wiley.com).

DOI 10.1002/hep.20048

Table 1. Primers Used in RT-PCR Assay

	Sense Primer	Antisense Primer	Product Size (bp)
ANG2	5′-GACGGCTGTGATGATAGAAATAGG-3′	5′-GACTGTAGTTGGATGATGTGCTTC-3′	264
ANG1	5′-AAATGGAAGGAAAACACAAGGAA-3′	5′-ATCTGCACAGTCTCTAAATGGT-3′	266
TIE2	5′-ATCCCATTTGCAAAGCTTCTGGCTGGC-3′	5′-TGTGAAGCGTCTCACAGGTCCAGGATG-3′	512
VEGF	5′-AAGCCATCCTGTGTGCCCCTGATG-3′	5′-GCGAATTCCTCCTGCCCGGCTCAC-3′	447, 375, 243
β-actin	5′-GAAAATCTGGCACCACACCTT-3′	5′-GTTGAAGGTAGTTTCGTGGAT-3′	590

Abbreviation: bp, base pair.

genesis. Of the four currently known Ang molecules (Ang-1, Ang-2, Ang-3, and Ang-4), the best-characterized ones are Ang-1 and its natural antagonist, Ang-2. Ang-1 is widely expressed in normal adult tissue,[11] whereas Ang-2 is expressed primarily at sites of vascular remodeling, such as the ovaries, uterus, and placenta.[10] Angiogenesis requires migration and remodeling of ECs derived from preexisting blood vessels and regulation of the perivascular microenvironment. Ang-2 destabilizes preexisting vessels by weakening interactions between ECs and periendothelial supporting cells (PESCs).[10,12] Ang-1 subsequently acts, via the Tie-2 receptor, to remodel these primitive vessels and to help maintain and stabilize mature vessels.[9,13]

Ang-2 is expressed in several types of human malignancies, including carcinomas of the colon, liver, stomach, lung, and thyroid, as well as malignant glioma.[14-21] Furthermore, gene transduction studies have demonstrated that forced expression of the *ANG2* gene in gastric and colon carcinoma cells is associated with increased vessel density.[16,22] These findings suggest that Ang-2 may be involved in tumor-associated neovascularization. Nonetheless, expression of Ang-2 in CRC metastases in the liver has not been fully characterized.

Although CRC metastatic to the liver is considered to be a hypovascular lesion (in contrast to hypervascular hepatocellular carcinoma), it appears that the periphery of the metastatic lesion retains rich vascularity.[23,24] We have examined the expression of *ANG2* RNA in CRC metastases in the liver and compared the results with those observed in primary CRC tissue samples using the reverse-transcription polymerase chain reaction (RT-PCR) assay. Using laser capture microdissection (LCM), RNA content data on *ANG2*, *ANG1*, *TIE2*, and the *VEGF* gene, which encodes the putative angiogenic factor VEGF (vascular endothelial growth factor), were obtained for normal liver cells and for metastatic CRC cells in the liver, with reference to vessel density in each region of the liver. Our results represent notable findings regarding tumor-associated neovascularization in CRC metastases in the liver and the possible link between this neovascularization and the concurrent expression of Ang-2 and VEGF.

Materials and Methods

Clinical Samples. Surgical specimens were obtained from patients who had undergone colectomy and/or hepatectomy at the Department of Surgery and Clinical Oncology at Osaka University (Osaka, Japan) between 1995 and 2001 because of CRC ($n = 36$) and/or CRC metastatic to the liver ($n = 14$; 8 solitary lesions and 6 multiple lesions). Nine liver metastases were found simultaneously with primary CRC (synchronous lesions), and 5 liver metastases were found at least 1 year after detection of primary CRC (metachronous lesions). Metastatic CRC lesions ranged in size from 1.0 to 7.0 cm (mean ± standard deviation, 3.1 ± 1.9 cm). None of the patients had been treated preoperatively with chemotherapy or radiotherapy. All resected surgical specimens were fixed with 10% buffered formalin. A portion of each tissue sample promptly was frozen in liquid nitrogen for the RT-PCR assay or for Western blot analysis. Of the 14 CRCs metastases of the liver, 10 were determined to be of sufficient quantity and were made into optimal cutting temperature compound–frozen samples.

RNA extraction. Total RNA was extracted from clinical samples and cell pellets via a single-step method using Trizol reagent (Life Technologies, Gaithersburg, MD), and complementary DNA (cDNA) was generated using avian myeloblastosis virus reverse transcriptase (Promega, Madison, WI) as described previously.[25]

LCM. Frozen tissue samples embedded in optimal cutting temperature compound were sectioned at 8 μm, mounted on uncoated glass slides, fixed with 70% ethanol for 10 minutes, and then washed with distilled water for 30 seconds. Sections were stained rapidly with hematoxylin-eosin (HE) solution, washed twice with 95% ethanol and once with 100% ethanol, and then washed with xylene. After 20 minutes of air-drying, LCM was performed using the LM200 LCM system (Arcturus Engineering, Santa Clara, CA). Sections were covered with transfer film (CapSure TF-100; Arcturus Engineering), and the targeted cell population was dissected with the laser beam and captured onto the film. The RNeasy minikit (Qiagen, Hilden, Germany) was used to extract a minimal amount

Table 2. RT-PCR Assay Conditions

	Amount of Each Primer Used (pmol)	β-Actin (pmol)	Denaturing Cycle	PCR Cycle	Extension Cy
ANG2	5	1	95°C, 12 min	95°C, 1 min; 53°C, 1 min; and 72°C, 1 min, × 35 cycles	72°C, 10 mi
ANG1	5	0.25-0.5	95°C, 12 min	95°C, 1 min; 51°C, 1 min; and 72°C, 1 min, × 37-40 cycles	72°C, 10 mi
TIE2	10	0.5	95°C, 12 min	95°C, 1 min; 58°C, 1 min; and 72°C, 1 min, × 43 cycles	72°C, 10 mi
VEGF	5	1.25	95°C, 12 min	95°C, 1 min; 58°C, 1 min; and 72°C, 1 min, × 35 cycles	72°C, 10 mi

of RNA from each tissue sample, as described previously.[26]

Semiquantitative duplex. RT-PCR. Semiquantitative analyses of the expression of *ANG1*, *ANG2*, *TIE2*, and *VEGF* RNA were performed using the duplex RT-PCR technique, as described previously.[25,27] β-actin was used as the internal standard. The sequences of the PCR primers and the sizes of the amplicons are shown in Table 1. PCR reactions were performed in a total volume of 25 μL, which consisted of 2 μL cDNA template, 1X Perkin-Elmer PCR buffer (Perkin-Elmer, Foster City, CA), 1.5 mM $MgCl_2$, 0.8 mM deoxynucleotide triphosphates, appropriate amounts of β-actin and each primer, and 1 unit Taq DNA Polymerase (AmpliTaq Gold; Roche Molecular Systems, Branchburg, NJ). The amounts of each primer and β-actin primer used and the PCR conditions are shown in Table 2. PCR amplification was performed with a Genamp PCR System 9600 (Perkin-Elmer, Foster City, CA).

Reagents. The anti-human antibodies used in the study were goat polyclonal Ang-1 antibody (Santa Cruz Biotechnology, Santa Cruz, CA), goat polyclonal Ang-2 antibody (Santa Cruz Biotechnology), rabbit polyclonal Tie-2 antibody (Santa Cruz Biotechnology), rabbit polyclonal VEGF antibody (Santa Cruz Biotechnology), mouse monoclonal CD31 antibody (Dako, Carpinteria, CA), mouse monoclonal α-SMA (smooth muscle actin) antibody (Dako), and rabbit polyclonal actin antibody (Sigma, St. Louis, MO). The blocking peptides that were used as immunogens for generation of the Ang-1 antibody and the Ang-2 antibody were obtained from Santa Cruz Biotechnology.

HE staining and immunohistochemistry. Paraffin sections measuring 4 μm in thickness were deparaffinized in xylene and rehydrated and stained with HE solution for histopathologic examination. Immunohistochemical analysis of CD31, Ang-2, and VEGF was performed using the Vectastain avidin-biotin complex peroxidase kit (Vector Laboratories, Burlingame, CA), as described previously.[25–27] Heat antigen retrieval was performed in 10 mM citrate buffer, pH 6.0, at 95 °C for 40 minutes. Primary antibodies were applied to sections at dilutions of 1:500 for CD31, 1:50 for Ang-2, and 1:50 for VEGF. As a positive control for Ang-2 staining, human placenta was used.[10,28] For the negative control, nonimmunized immunoglobulin G (Vector Laboratories) was used as a substitute for the primary antibody.

Vessel Counts. Blood vessels were counted with a microscope at 200× magnification after immunostaining the vascular ECs with anti-CD31 antibody. Ten visual fields were randomly selected in each portion of the metastatic CRC lesion (*i.e.*, the periphery, the intermediate region, and the center), and vessel counts per mm^2 were calculated. For evaluation of vessel diameter in the short

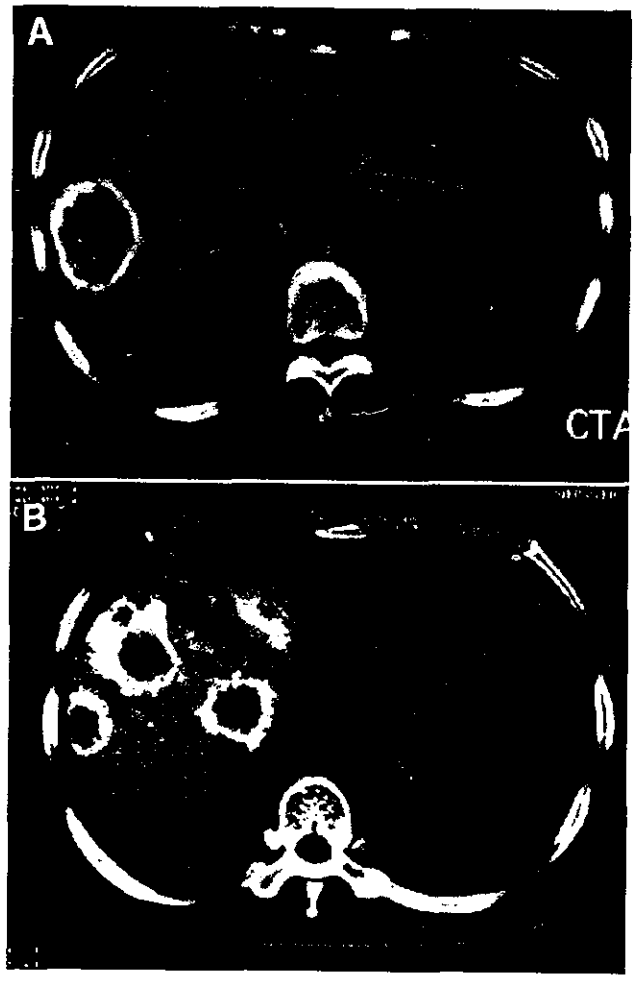

Fig. 1. Computed tomography-arteriography. Computed tomograp scanning was performed during infusion of contrast media into t common hepatic artery. Liver metastases from CRC showed a typi ringlike enhancement pattern around the tumor. Two representati cases (A and B) are shown.

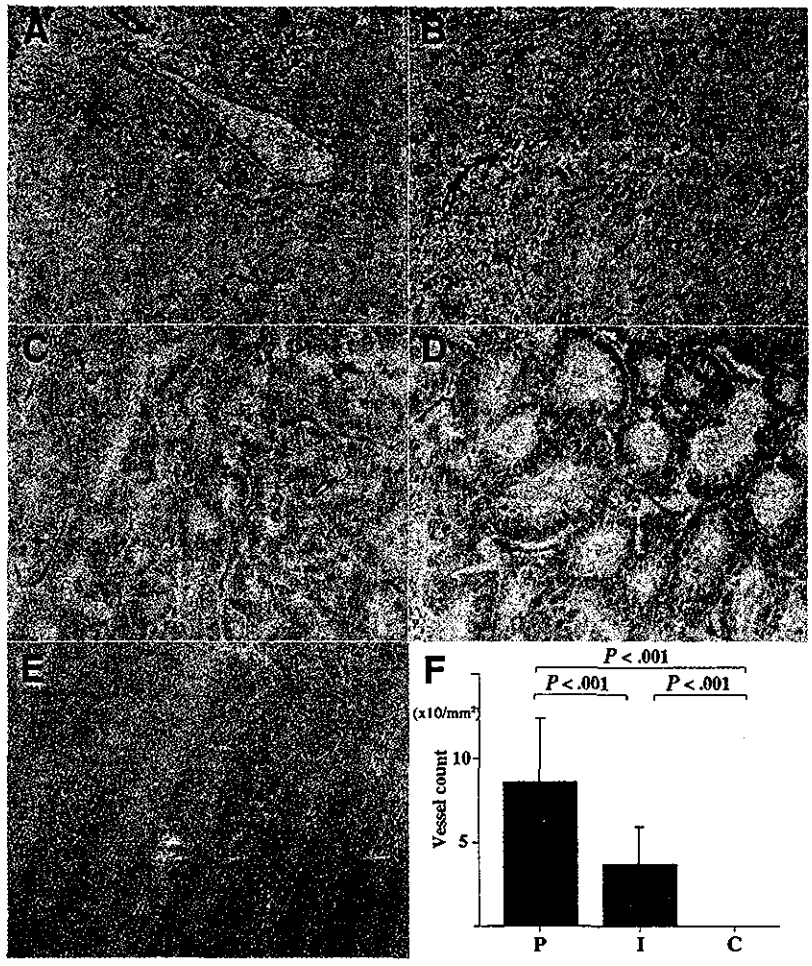

Fig. 2. Immunohistochemical analysis of CD31-positive vascular ECs. (A) Normal liver tissue far from the metastatic lesion. Positive immunoreactivity for CD31 was noted only in vascular ECs within the Glisson's triangle area. (B) Liver region adjacent to the metastatic colorectal tumor. Large vessels were abundant. (C) Periphery of the metastatic colorectal tumor. Tumor vessels frequently are present in the peripheral region. Tumor cells generally were viable. (D) Intermediate region of the metastatic colorectal tumor. Tumor vessels are less abundant. (E) Central region of the metastatic colorectal tumor. Note the presence of necrotic tumor cells and the lack of vessels. (F) Vessel counts in metastatic CRC in the liver (P, periphery; I, intermediate region; C, central region). There was a significant decrease in vessel count going from the periphery to the intermediate portion of the tumor, and also going from the intermediate portion to the center. $P < .001$ for each pair of adjacent regions. (E: original magnification ×100.)

direction, more than 50 vessels were measured using Mac Scope Software (Mitani Corp., Fukui, Japan).[27]

Vessel maturation. Vessel maturation was defined as the extent of recruitment of PESCs around ECs and was expressed as the percentage of encirclement of vessel outline with α-SMA-expressing PESCs.[10,13,16,21] Thus, double-staining of ECs and PESCs was performed with anti-CD31 antibody and anti-α-SMA antibody, respectively. In brief, CD31 staining, which yields a brown color, was performed. After removal of the CD31 antibody by thorough washing in 0.1 M glycine solution, pH 2.2, for 1 hour, mouse monoclonal anti-human α-SMA antibody at a dilution of 1:200 was applied to the section for 2 hours at room temperature. This step was followed by incubation with anti-mouse secondary antibody conjugated with a dextran backbone containing alkaline phosphatase (EnVision AP; Dako) for 30 minutes. Color development (deep pink) based on alkaline phosphatase activity was achieved using fuchsin solution. For quantification, 10 blood vessels in each portion of the lesion were randomly selected under the microscope at 200× magnification and evaluated for maturation index.

Cell cultures. Human colon cancer cell lines HCT116, SW480, and DLD1 were obtained from the American Type Culture Collection (Manassas, VA). These cells were grown in Dulbecco's modified Eagle's medium supplemented with 10% fetal bovine serum, 100 units/mL penicillin, and 100 μg/mL streptomycin at 37 °C in a humidified incubator with 5% CO_2 in air. Human umbilical vein ECs were grown on MCDB131 culture medium (Chlorella Inc., Tokyo, Japan) supplemented with 10% fetal bovine serum, antibiotics, and 10 ng/mL fibroblast growth factor.

Western blot analysis. Approximately 50 mg of each sample (3×10^6 cells) was homogenized in 0.5 mL RIPA

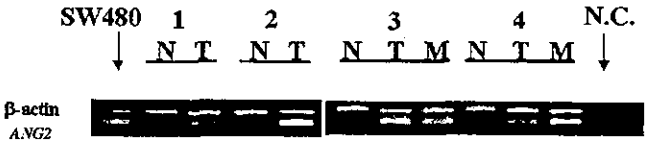

Fig. 3. Expression of *ANG2* RNA in clinical samples. Expression of *ANG2* RNA was examined by RT-PCR in normal mucosa (N), CRC tissue (T), and metastatic CRC in the liver (M). Expression of *ANG2* RNA was graded as absent, weak, or strong. Numbers represent different cases (Cases 1-2, paired normal mucosa and CRC tissues; Cases 3-4, CRC cases with simultaneous liver metastases). The housekeeping gene encoding β-actin served as an internal control for RNA quality. The sizes of the amplicons for *ANG2* and β-actin were 264 and 590 base pairs, respectively. SW480 colon cancer cells served as positive controls for *ANG2* RNA expression. N.C., negative control (no RNA extract).

buffer (25 mM Tris, pH 7.4; 50 mM NaCl; 0.5% sodium deoxycholate; 2% NP-40; and 0.2% sodium dodecyl sulfate) with protease inhibitors (1 mM phenylmethylsulfonyl fluoride, 10 μg/mL aprotinin, and 10 μg/mL leupeptin). The homogenate was centrifuged at 14,000 revolutions per minute for 20 minutes at 4°C. The resulting supernatant was collected, and the total protein concentration was determined using the Bradford protein assay (Bio-Rad, Hercules, CA). Western blotting was performed as described previously.[25] In brief, 50 μg of protein was subjected to sodium dodecyl sulfate-polyacrylamide gel electrophoresis on 7.5%–12.5% gels. Protein samples then were transferred onto a polyvinylidene difluoride membrane. After blocking in 5% skim milk, the membrane was incubated with the appropriate primary antibody for 1 hour at 4°C using the following concentrations: anti-Ang-1, 1 μg/mL; anti-Ang-2, 1 μg/mL; anti-VEGF, 1 μg/mL; anti-Tie-2, 1 μg/mL; and anti-β-actin, 1:1000 dilution. This step was followed by

Table 3. Association Between Clinicopathologic Features and ANG2 mRNA Expression in Primary Cancer Tissue Samples

	ANG2 Expression		
	Absent or Low	High	*P* Value
Sex			
Male	9	9	NS
Female	4	14	
Age (yrs)	59.1 ± 12.9	60.4 ± 12.7	NS
Tumor location			
Colon	11	12	NS
Rectum	2	11	
Tumor size* (cm)	4.42 ± 2.85	6.06 ± 2.15	0.023
Depth of infiltration			
~mp	2	1	NS
ss~	11	22	
Lymphatic involvement			
Yes	9	20	NS
No	4	3	
Vascular involvement			
Yes	3	10	NS
No	10	13	
Lymph node metastasis			
Present	2	13	0.033
Absent	11	10	
Dukes' stage			
A, B	7	8	NS
C, D	6	15	

Abbreviations: NS, not significant; mp, muscularis propria; ss, subserosa.
*Diameter, 2.4-11.3 cm (mean, 5.5 ± 2.1 cm).

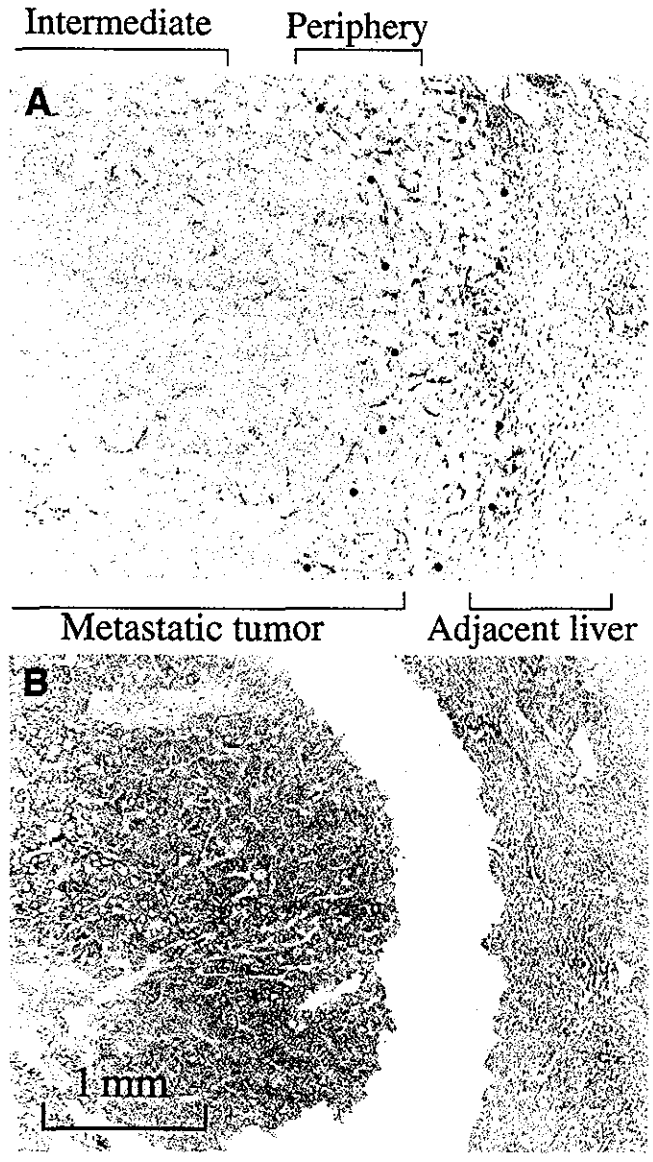

Fig. 4. Vascularity of metastatic CRC in the liver and LCM analysis. (A) CD31-stained section of a metastatic CRC lesion in the liver. Abundant tumor vessels are present in the peripheral region of the tumor. The number of tumor vessels decreased in the intermediate region. CD31 staining of the liver tissue adjacent to the metastatic CRC lesion reveals dilated sinusoids with capillarization.[5,42] (B) LCM was performed to obtain RNA extracts from the liver tissue adjacent to the metastatic CRC lesion, the periphery of the lesion, and the intermediate portion of the lesion. The peripheral portion was excised from a section that was lightly stained with eosin, with reference to a serial section stained with anti-CD31 antibody. (Original magnification ×40.)

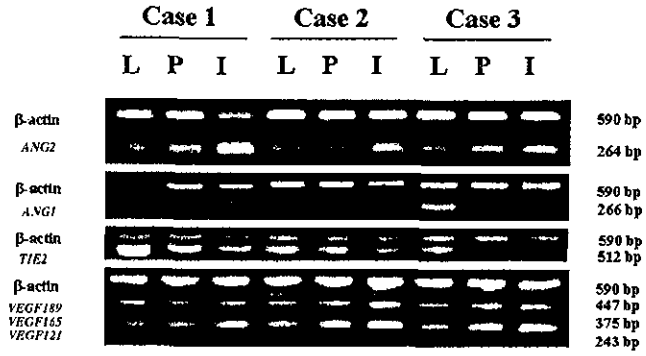

Fig. 5. Expression of RNA encoding Ang-2 and related molecules in metastatic CRC in the liver. The levels of RNA encoding Ang-2 and related molecules were examined using semiquantitative RT-PCR after LCM. Expression of *ANG2* RNA, but not *ANG1* RNA, was greater within the metastatic CRC lesion than in the bordering liver tissue. In particular, *ANG2* RNA expression was evident in the intermediate region of the tumor. Higher expression of *TIE2* RNA was observed in the bordering liver tissue than in the metastatic CRC lesion. In the analysis of *VEGF* expression, three isoforms, VEGF-121, VEGF-165, and VEGF-189, were considered. In each tumor region, the expression of *VEGF* RNA was similar to the expression of *ANG2* RNA. L, liver region adjacent to the metastatic CRC lesion; P, periphery of the metastatic CRC lesion; I, intermediate region of the metastatic CRC lesion; bp, base pair.

incubation with the corresponding secondary antibody at a dilution of 1:2000–4000. For detection of the immunocomplex, the Amersham enhanced chemiluminescence detection system (Amersham, Arlington Heights, IL) was used. Protein lysates from human umbilical vein ECs and colon cancer cells served as positive controls for Tie-2 and VEGF, respectively.[29–32]

Statistical analysis. Statistical analysis was performed using StatView J-5.0 software (Abacus Concepts, Berkeley, CA). Data are expressed as mean values ± standard deviations. Associations between discrete variables were assessed using Fisher's exact test. Mean values were compared using the Student's *t* test. The Wilcoxon signed rank test was used to evaluate differences among corresponding objects. Correlation significance was assessed using Pearson's correlation coefficient test. $P < .05$ was taken to indicate that a given correlation was significant.

Results

Vascularity of CRC Metastases in the Liver. On computed tomography–arteriography, all metastatic CRCs ($n = 14$) exhibited ring enhancement, suggesting the presence of an abundant blood supply around the tumors (Fig. 1). Staining of vascular ECs with anti-CD31 antibody was performed to assess the vascular density of the liver tissue and the metastatic CRC. Although positive immunoreactivity for CD31 was noted only in vascular ECs in the Glisson's triangle area (Fig. 2A) and in the central vein in the distant normal liver tissue, there were numerous large blood vessels (diameter [mean ± standard deviation], 51.9 ± 13.6 μm) with positive immunoreactivity in the liver region adjacent to the metastatic CRC (Fig. 2B). Within the metastatic CRC, high vascularity involving short, tortuous blood vessels measuring 28.2 ± 11.6 μm in diameter was observed at the periphery (Fig. 2C), but virtually no CD31-positive ECs were present in the central region (Fig. 2E). The intermediate region between the periphery and the central part of the tumor exhibited intermediate vascularity (Fig. 2D). These tumor vascularity features were observed in all CRC metastases in the liver that were examined. Blood vessel counts were estimated to be 75.5 ± 32.6 per mm^2 in the periphery, 33.4 ± 18.2 per mm^2 in the intermediate region, and 0 ± 0 per mm^2 in the central region (Fig. 2F). There was a significant decrease in vessel count going from the periphery of the tumor to the intermediate region, and also

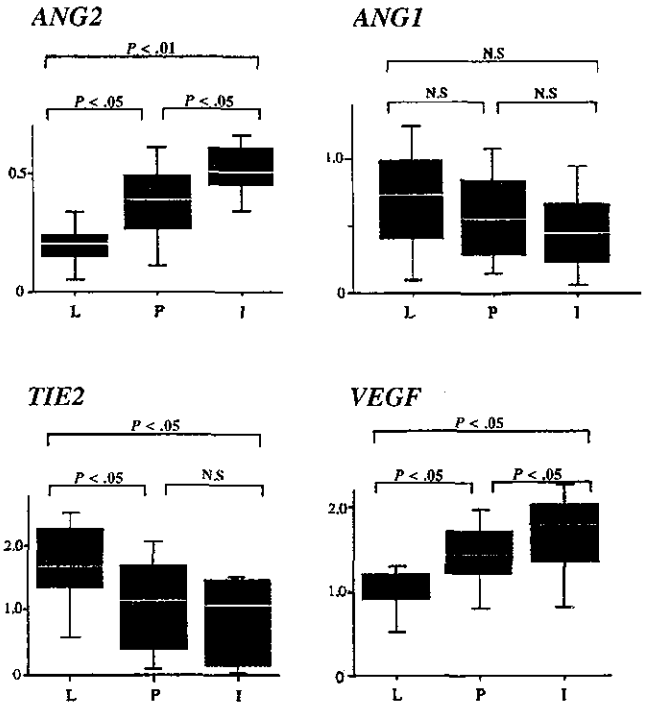

Fig. 6. Expression of RNA encoding Ang-2, Ang-1, Tie-2, and VEGF in each tumor region. All RNA expression levels were normalized to β-actin. Data are displayed in box plots, with mean values represented by the horizontal lines inside the boxes. Mean values were as follows: *ANG2*: liver, 0.20 ± 0.10; periphery, 0.38 ± 0.18; intermediate region, 0.51 ± 0.11; *ANG1*: liver, 0.67 ± 0.42; periphery, 0.56 ± 0.34; intermediate region, 0.47 ± 0.32; *TIE2*: liver, 1.66 ± 0.72; periphery, 1.09 ± 0.76; intermediate region, 0.87 ± 0.59; *VEGF*: liver, 0.96 ± 0.28; periphery, 1.39 ± 0.41; intermediate region, 1.62 ± 0.58. The Wilcoxon signed rank test indicated a significant increase in *ANG2* and *VEGF* RNA expression between each pair of adjacent regions. The level of *TIE2* RNA expression was significantly higher in bordering liver tissue than in the peripheral and intermediate tumor regions. L, liver region adjacent to the metastatic CRC lesion; P, periphery of the metastatic CRC lesion; I, intermediate region of the metastatic CRC lesion.

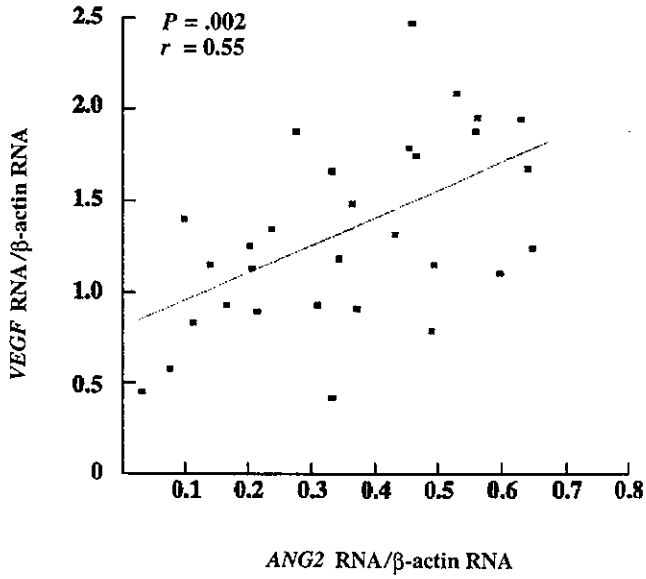

Fig. 7. Correlation between *VEGF* and *ANG2* RNA expression in liver metastases. Thirty dissected samples were examined for a correlation between *VEGF* and *ANG2* RNA levels. A significant correlation ($P = .002$) was indicated by Pearson's correlation coefficient test when the sample number was 30 (correlation coefficient: $r = 0.55$).

going from the intermediate region to the center of the tumor ($P < .001$ for each pair of adjacent regions).

ANG2 RNA content in clinical samples. *ANG2* RNA was expressed in 7 of 36 normal mucosae (19.4%), 30 of 36 primary CRCs (83.3%), and 14 of 14 CRC metastases in the liver (100%). *ANG2* RNA bands were absent, weak, or strong, whereas β-actin RNA bands were relatively uniform (Fig. 3). High expression of *ANG2* RNA (defined by a band density of *ANG2* relative to β-actin of > 2) was noted in 3 of 36 normal mucosae (8.3%), 23 of 36 CRCs (63.9%), and 14 of 14 CRC metastases in the liver (100%). Thus, high expression of *Ang2* RNA was significantly more common in metastatic CRC than in normal mucosa ($P < .0001$) or primary CRC ($P = .024$). Clinicopathologic investigation of primary CRC revealed that larger tumors ($P = .023$) and the presence of lymph node metastases ($P = .033$) were significantly associated with high *ANG2* RNA expression (Table 3).

Content of RNA encoding Ang-2 and related molecules in CRC metastases in the liver. To explore the distribution of cells producing modifiers of angiogenesis (Ang-1, Ang-2, Tie-2, and VEGF), optimal cutting temperature compound–embedded frozen samples of CRC metastases in the liver were dissected via LCM so that RNA could be extracted. Based on CD31 staining results (Fig. 4A), we defined the periphery of the metastatic CRC lesion as the region in which tumor-associated vessels were abundant, and we defined the intermediate region as the area in which tumor-associated vessels were noticeably less abundant. Each region was dissected on eosin-stained serial section (Fig. 4B), but the central region of the tumor was not dissected, because it typically was necrotic. For comparison, the liver region adjacent to the metastatic CRC lesion also was dissected.

ANG2 RNA expression was stronger within the metastatic CRC lesion compared with the bordering liver region. In particular, *ANG2* RNA expression in the intermediate region was evident in several cases (Fig. 5; Cases 1–3). Densitometric analysis indicated that there was an increase in *ANG2* RNA content going from bordering liver to the tumor periphery, and also going from the periphery to the intermediate region of the tumor ($P < .05$ for each pair of adjacent regions) (Fig. 6). High expression of *ANG1* RNA in the bordering liver region rather than within the metastatic CRC lesion was observed in some cases (Fig. 5; Case 3), but statistical analysis indicated no significant difference between adjacent regions (Fig. 6). High expression of *TIE2* RNA was more common in the bordering liver region than within the metastatic CRC lesion (Fig. 5). Statistical analysis indicated that the *TIE2* RNA content in bordering liver tissue was significantly greater than the content in the peripheral and intermediate regions of the tumor (Fig. 6; $P < .05$ in each case). In the analysis of *VEGF* RNA content, three isoforms, VEGF-121, VEGF-165, and VEGF-189, were considered. When all 3 isoforms were taken into account, there was a significant increase in *VEGF* RNA content going from bordering liver to the tumor periphery, and also going from the periphery to the intermediate region of the tumor (Fig. 6; $P < .05$ for each pair of adjacent regions). Considered separately, expression of RNA encoding VEGF-165 and expression of RNA encoding VEGF-121 also increased in similar patterns (data not shown). Expression of RNA encoding VEGF-189 was not quantifiable in some samples.

Because similar expression patterns were observed for *VEGF* and *ANG2* (Fig. 6), we analyzed the correlation between *VEGF* RNA expression and *ANG2* RNA expression. When *VEGF* expression data were plotted against *ANG2* expression data ($n = 30$; 3 dissected portions from each of 10 samples) (Fig. 7), a significant correlation was noted ($r = 0.55$; $P = .002$).

Expression of Ang-2/ANG2 and related molecules/genes at the protein and RNA levels. Using three colon cancer cell lines and four nonneoplastic colonic mucosa/primary CRC tissue pairs, protein expression of Ang-1, Ang-2, Tie-2, and VEGF was examined by Western blot analysis, and the results of this analysis were compared with the corresponding RNA expression results. With respect to the extent of expression by each of the three cell lines and the relative expression levels in normal mucosa and pri-

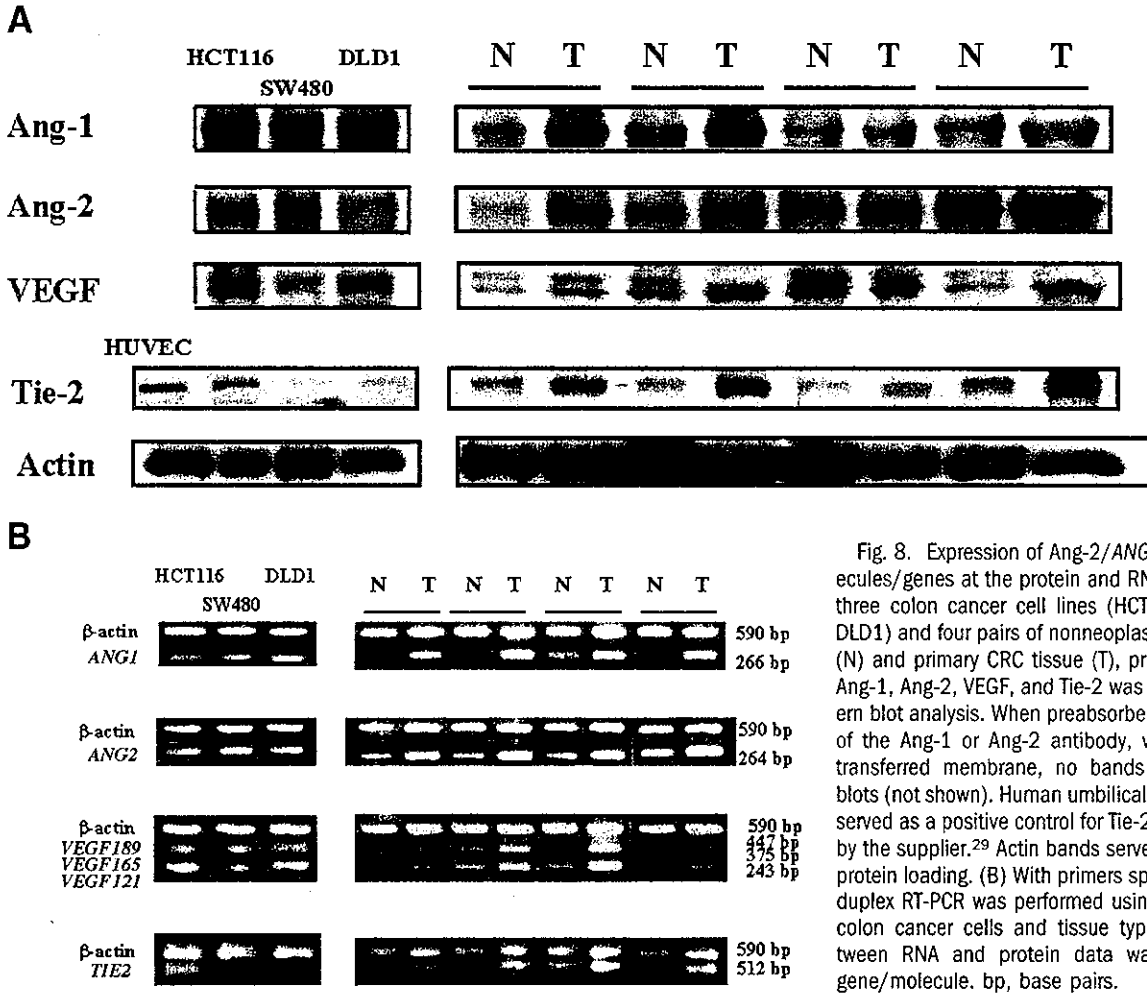

Fig. 8. Expression of Ang-2/*ANG2* and related molecules/genes at the protein and RNA levels. (A) Using three colon cancer cell lines (HCT116, SW480, and DLD1) and four pairs of nonneoplastic colonic mucosa (N) and primary CRC tissue (T), protein expression of Ang-1, Ang-2, VEGF, and Tie-2 was examined by Western blot analysis. When preabsorbed antibody, instead of the Ang-1 or Ang-2 antibody, was applied to the transferred membrane, no bands appeared on the blots (not shown). Human umbilical vein ECs (HUVECs) served as a positive control for Tie-2, as recommended by the supplier.[29] Actin bands served as references for protein loading. (B) With primers specific to each RNA, duplex RT-PCR was performed using the same sets of colon cancer cells and tissue types. Agreement between RNA and protein data was noted for each gene/molecule. bp, base pairs.

mary CRC tissue, good agreement was noted for each molecule and corresponding gene at the protein and RNA levels (Fig. 8A,B).

Immunohistochemical analysis of Ang-2 in CRC metastases in the liver. Immunohistochemical analysis of Ang-2 was performed on 14 paraffin-embedded samples of CRC metastases in the liver. The control section of human placental tissue exhibited positive staining for Ang-2 (Fig. 9A). Liver tissue adjacent to the metastasis generally exhibited weak-to-moderate staining (Fig. 9B), whereas most metastatic CRCs (12 of 14) exhibited moderate-to-strong staining for Ang-2. A gradual increase in expression of the Ang-2 protein going from the periphery to the intermediate region of the metastatic tumor was observed in 11 of 14 cases (Fig. 9C,D). Overall, Ang-2 immunostaining results were well correlated with the corresponding RT-PCR results (data not shown). VEGF staining yielded similar results to those observed for Ang-2 staining (data not shown).

Maturation of blood vessels. For assessment of the extent of vessel maturation, double-staining for CD31 and α-SMA was performed to detect ECs and PESCs, respectively. Figure 10 shows representative vessels in each tumor region. Mature vessels, such as the portal vein and the hepatic artery, were virtually surrounded by PESCs (Fig. 10A). Within the metastatic CRC lesion, a number of myofibroblastlike cells also expressed α-SMA in the stroma. Vessels at the periphery partially lacked α-SMA expression derived from PESCs (Fig. 10B). Vessels located in the intermediate region were surrounded by PESCs to a lesser extent compared with vessels in the tumor periphery (Fig. 10C). Quantitative analysis indicated that the vessel maturation index was 100% ± 0% in bordering liver, 87.6% ± 20.1% in the tumor periphery, and 64.2% ± 28.1% in the intermediate region of the tumor (Fig. 10D). The difference between each pair of regions was statistically significant ($P < .01$).

Discussion

Using computed tomography–angiography and histopathologic methods, we observed abundant tumor vessels at the periphery of the metastatic tumor, where tumor cells generally were viable. In contrast, the center of the

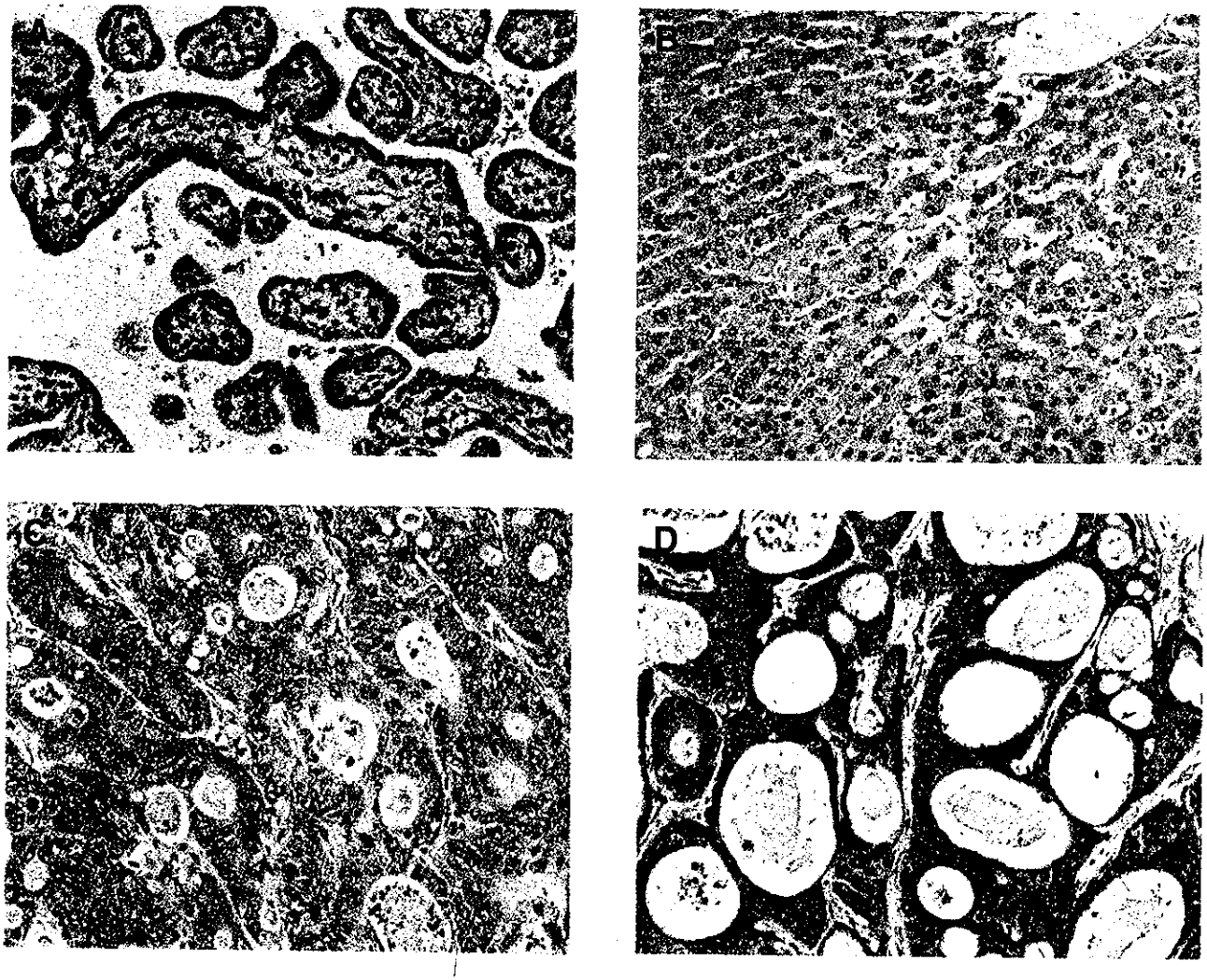

Fig. 9. Immunohistochemical analysis of Ang-2 in metastatic CRC in the liver. (A) The control section of human placental tissue exhibited positiv staining for Ang-2 in trophoblast. (B) Liver tissue adjacent to the metastatic lesion generally exhibited weak staining. A gradual increase in expressio of Ang-2 going from (C) the tumor periphery to (D) the intermediate region of the tumor commonly was noted. Most metastatic CRCs (12 of 14 exhibited moderate-to-strong expression of Ang-2. (Original magnification ×100.)

metastatic lesion was devoid of CD31-positive tumor vessels and consisted of a considerable amount of necrotic tissue. These findings suggest that tumor angiogenesis at the frontier of the metastatic CRC lesion in the liver may be essential to the consistent growth of malignant cells.

Although it is unknown whether Ang-2 is involved in neovascularization of metastatic CRC, the data from the current study suggest that this may be the case. First, RT-PCR assays indicated that high expression of *ANG2* RNA was more common in metastatic CRC tissue than in primary CRC tissue or normal colonic mucosa. Second, LCM analysis revealed that *ANG2* RNA was expressed in the peripheral and intermediate regions of metastatic CRC lesions, where tumor angiogenesis was present. In fact, *ANG2* RNA levels were higher in the peripheral and intermediate tumor regions than in the bordering liver tissue. Furthermore, some synchronous CRC metastases in the liver exhibited even higher *ANG2* RNA expression levels than did the primary CRCs from the corresponding patients (3 of 9 cases [33%]; data not shown).

Clinicopathologic assessment was useful in investigating the putative fundamental action of the *ANG2* gene in primary CRC. Our data indicated that, as in thyroid tumors,[18] larger primary CRCs had higher *ANG2* RNA expression levels. This result is consistent with the finding in recent *in vivo* studies that transduction of the *ANG2* gene into colon or gastric cancer cells produced larger tumors.[16,22] Because these enlarged xenografts exhibited an increased vessel count, it is believed that Ang-2 produced by malignant cells may facilitate neovascularization and contribute to rapid malignant growth. Another notable finding was the positive association between high *ANG2* RNA expression and metastasis to the lymph nodes, suggesting a possible role for Ang-2 in metastatic spread.

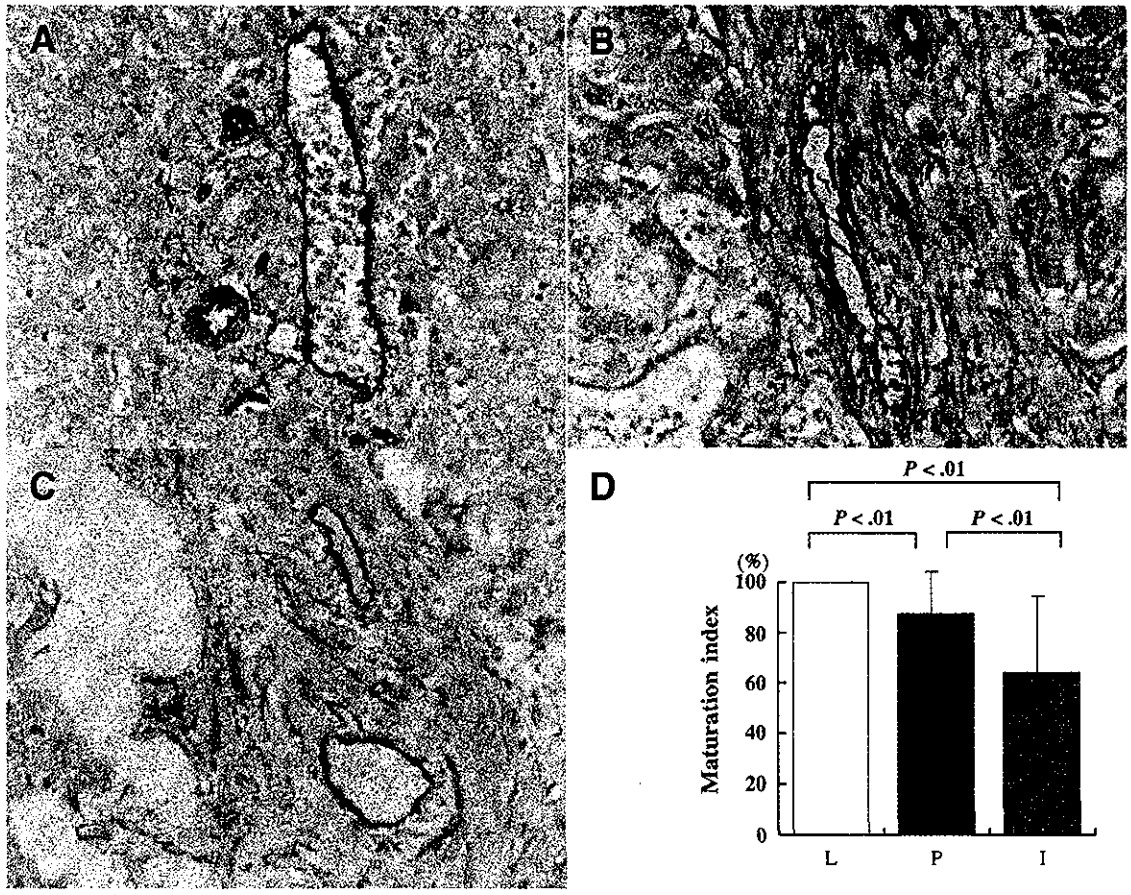

Fig. 10. Vessel maturation. ECs and PESCs were stained on the same section with anti-CD31 antibody and anti-α-SMA antibody, respectively, using the double-staining technique. Vessels were characterized by CD31 staining for ECs (brown). α-SMA staining (pink) was a marker for PESCs. (A) Mature vessels, such as the portal vein and the hepatic artery, were virtually surrounded by PESCs. (B) Vessels in the peripheral region of the metastatic CRC lesion in the liver partially lacked α-SMA expression derived from PESCs. A small number of α-SMA-positive myofibroblastlike cells also were present in the stroma. (C) In the intermediate region, vessels were surrounded by fewer PESCs. (D) The vessel maturation index was 100% ± 0% in adjacent liver tissue, 87.6% ± 20.1% in the tumor periphery, and 64.2% ± 28.1% in the intermediate region; all differences were significant ($P < .01$). L, liver region adjacent to the metastatic CRC lesion; P, periphery of the metastatic CRC lesion; I, intermediate region of the metastatic CRC lesion. (Original magnification ×200.)

Of several angiogenic factors (*e.g.*, beta fibroblast growth factor and platelet-derived endothelial cell growth factor), VEGF is the best-characterized proangiogenic agent that is known to be involved in the development of metastatic CRC in the liver.[30–32] The usefulness of anti-VEGF agents currently is being tested in clinical trials.[33] By using VEGF as a control in the current study, the relevance of Ang-2 in metastatic CRC in the liver was made more evident. The RNA expression pattern of *ANG2*, but not *ANG1*, was very similar to that of *VEGF* (Fig. 6), and we found a significant correlation between expression of *ANG2* RNA and expression of *VEGF* RNA in each tumor region (Fig. 7). Previous studies have demonstrated that Ang-2 promotes angiogenesis synergistically with VEGF in several *in vivo* models[10,13] and that coexpression of Ang-2 and VEGF often is observed in gastric cancer, glioma, thyroid cancer, and lung cancer.[16–18,21] Together, Ang-2 and VEGF may participate in tumor-associated angiogenesis in liver metastases.

Although RT-PCR assays provide data on gene expression at the RNA level, biologic function is carried out by proteins. Thus, insight into the expression of the angiogenesis-related proteins themselves would be desirable. There is evidence that expression of *VEGF* messenger RNA (mRNA) is well correlated with VEGF protein expression in human hepatocellular carcinoma.[34,35] It also has been reported that *ANG1*, *ANG2*, and *TIE2* RNA expression data were concordant with the corresponding protein expression data in human hepatocellular carcinoma and in rheumatoid arthritis.[35,36] We also found good agreement between RNA and protein expression data for the four angiogenesis-related molecules investigated (Fig. 8). Furthermore, immunohistochemical analysis provided confirmatory results regarding Ang-2 and VEGF expression in metastatic CRC. These findings suggest that expression of these proteins may be regulated at a transcriptional level.

The current study raised the question of why RNA expression of *ANG2* and *VEGF* increased going from the